

Symmetry-protected dissipative preparation of matrix product states

Leo Zhou,^{1,*} Soonwon Choi,^{1,*} and Mikhail D. Lukin¹

¹*Department of Physics, Harvard University, Cambridge, Massachusetts 02138, USA*

(Dated: June 8, 2017)

We propose and analyze a method for efficient dissipative preparation of matrix product states that exploits their symmetry properties. Specifically, we construct an explicit protocol that makes use of driven-dissipative dynamics to prepare the Affleck-Kennedy-Lieb-Tasaki (AKLT) states, which features symmetry-protected topological order and non-trivial edge excitations. We show that the use of symmetry allows for robust experimental implementation without fine-tuned control parameters. Numerical simulations show that the preparation time scales polynomially in system size n . Furthermore, we demonstrate that this scaling can be improved to $\mathcal{O}(\log^2 n)$ by using parallel preparation of AKLT segments and fusing them via quantum feedback. A concrete scheme using excitation of trapped neutral atoms into Rydberg state via Electromagnetically Induced Transparency is proposed, and generalizations to a broader class of matrix product states are discussed.

Entangled many-body states play a central role in understanding strongly correlated quantum matter and constitute the key resource for quantum information science. Matrix product states (MPS) [1] form an important class of many-body entangled states that can describe a variety of one dimensional quantum systems, including those featuring symmetry-protected topological (SPT) order [2]. Such states can be prepared either through a sequence of unitary quantum gate operations, or by first engineering the parent Hamiltonian and subsequently preparing its ground state via adiabatic evolution or cooling [3–9]. However, generating entanglement among a large number of particles using these approaches is challenging, as it requires high-fidelity control of interactions while maintaining low entropy for intrinsically out-of-equilibrium systems. In particular, unavoidable coupling to environment limits the lifetime of these states and hinders their potential applications.

In this paper, we propose and analyze an alternative method involving efficient dissipative preparation [10–17] of matrix product states by coupling to environment so that the desired state is obtained as the unique steady state of time evolution. While such approaches to prepare MPS have been described previously [10, 11], their implementations are typically challenging as they require engineering of complex interactions with environment. Here, we show how symmetries can be used to design a simple, translation-invariant dissipative process that only requires a single decay channel and global manipulations to create a desired MPS.

As a specific example, we describe a scheme to deterministically prepare a chain of spin-1 particles into the ground states of a gapped, frustration-free Hamiltonian

$$H_{\text{AKLT}} = \sum_i [\vec{S}_i \cdot \vec{S}_{i+1} + \frac{1}{3}(\vec{S}_i \cdot \vec{S}_{i+1})^2], \quad (1)$$

where \vec{S}_i is the spin-1 vector operator acting on a particle at site i . First studied by Affleck, Kennedy, Lieb, and Tasaki (AKLT), the ground state of H_{AKLT} is an example

of MPS and a model state for the Haldane phase [18–20]. While under periodic boundary condition, H_{AKLT} has a unique ground state; under open boundary condition, the ground states are 4-fold degenerate due to two fractionalized degrees of freedom on the edges. These constitute a signature of topological order, which can be experimentally verified by measuring a non-local string order parameter [21, 22].

Our approach makes use of $\text{SO}(3)$ spin-rotation symmetry of the parent Hamiltonian H_{AKLT} for preparation of an exact AKLT state. By converting the energy penalties imposed by H_{AKLT} into dissipative penalties in the form of decay channels, we can engineer a process that effectively cools to the ground states. More specifically, we start with a dissipative dynamics that eliminates one type of excitations in H_{AKLT} . Then, all other types of excitations can be eliminated using global spin-rotations. Since these rotations belong to a continuous symmetry of H_{AKLT} , their implementations are robust against imperfections in control parameters such as durations, phases, or strengths of electromagnetic driving. Using numerical simulations, we find that the state-preparation time scales polynomially with the system size n . We further show how this scaling can be improved to $\mathcal{O}(\log^2 n)$ by first preparing multiple spin chains in parallel and then connecting them via repeated measurements with feedback. This corresponds to an exponential improvement over $\mathcal{O}(n^{\log n})$ in a previous work [11]. As an example, we show that our protocol can be readily implemented in a system of trapped neutral atoms [23–25] using Rydberg-EIT mechanism [26]. This strategy generalizes to a broader class of MPS that includes the ground states of SPT phases.

Dissipative dynamics.— We consider a Markovian driven-dissipative dynamics described by the following Liouvillian \mathcal{L} :

$$\dot{\rho} = \mathcal{L}\rho \equiv -i[H, \rho] + \sum_{\mu} \Gamma_{\mu} \mathcal{D}[c_{\mu}]\rho, \quad (2)$$

where ρ is density operator of a system, H is a Hamilto-

nian governing coherent dynamics, and $\mathcal{D}[c_\mu]\rho \equiv c_\mu \rho c_\mu^\dagger - \{c_\mu^\dagger c_\mu, \rho\}/2$ characterizes incoherent dynamics by jump operators c_μ at rate Γ_μ . The dynamics of \mathcal{L} can be understood as the system evolving with a non-Hermitian Hamiltonian $H_{\text{eff}} = H - i \sum_\mu \Gamma_\mu c_\mu^\dagger c_\mu / 2$, while stochastically undergoing quantum jumps $\rho \mapsto c_\mu \rho c_\mu^\dagger$ at rates $\text{tr}[\Gamma_\mu c_\mu^\dagger c_\mu \rho]$ for each jump operator [27].

Our construction of \mathcal{L} exploits the $\text{SO}(3)$ symmetry that conserves the total angular momentum. In particular, each term in H_{AKLT} can be written as $2P_i - 2/3$, where P_i is the projection operator onto the subspace of total angular momentum $J_i = S_i + S_{i+1} = 2$ for the pair of spins at site i and $i + 1$. Hence, the energy is minimized by a state $|G\rangle$ if it has no population in the $J_i = 2$ manifold, i.e. $P_i |G\rangle = 0$, for every nearest neighboring pair. Under open boundary condition, there are four such states $|G_{ab}\rangle$, labelled by two spin-1/2 edge degrees of freedom $a, b \in \{\uparrow, \downarrow\}$. Under periodic boundary condition, only a unique state $|G_\circ\rangle \propto |G_{\uparrow\uparrow}\rangle + |G_{\downarrow\downarrow}\rangle$ satisfies this condition [28]. Below, we use $|G\rangle$ to denote the ground state(s) when the boundary condition is not specified.

In order to prepare $|G\rangle$, we use jump operators to depopulate $J_i = 2$ manifold of every neighboring pair. For example, we can set $H = 0$ and use five different types of jump operators,

$$c_m^{(i)} = |\phi_m\rangle \langle J = 2, J^z = m |_{i, i+1}, \quad (3)$$

where $\{|J = 2, J^z = m\rangle_{i, i+1} : m = -2, \dots, 2\}$ is an orthonormal basis that spans the $J_i = 2$ manifold for the pair at site i and $i + 1$, and $|\phi_m\rangle$ is any other quantum states with non-zero population in $J_i = 0, 1$ manifolds, i.e., $\langle \phi_m | P_i | \phi_m \rangle < 1$. With these jump operators, quantum jumps occur at the rate

$$\Gamma_{\text{total}} = \Gamma \sum_{i, m} \text{tr} \rho c_m^{(i)\dagger} c_m^{(i)} = \Gamma \sum_i \text{tr} \rho P_i, \quad (4)$$

which vanishes only for ground state $|G\rangle$. This implies that $|G\rangle$ is a steady state of \mathcal{L} , and any other quantum state will undergo a series of quantum jumps. The absence of quantum jumps over sufficiently long time heralds a successful preparation of desired states.

Using $\text{SO}(3)$ symmetry, this construction can be effectively realized with only one type of jump operator via global coherent manipulations H . More specifically, let us consider a dynamics with only one jump operator, $c_2 = |00\rangle \langle J = 2, J^z = 2 | = |00\rangle \langle ++ |$, written in the S^z basis $\{|+\rangle, |0\rangle, |-\rangle\}$. After time evolution over duration $\tau/5$, we apply a fast, global pulse $V = \exp[i(2\pi/5) \sum_i S_i^y]$, rotating the entire spin ensemble by an angle $2\pi/5$ about the y -axis. In a rotating frame, this operation implements the jump operator $V^\dagger c_2 V$. Repeated multiple times, we obtain five distinct jump operators $\bar{c}_\alpha := (V^\dagger)^\alpha c_2 (V)^\alpha$ for $\alpha \in \{0, \dots, 4\}$ after the α -th (modulo 5) pulses. For sufficiently short

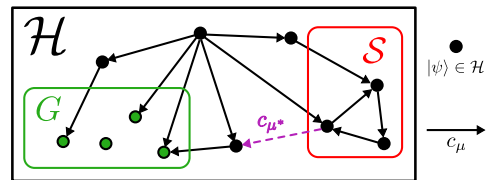


FIG. 1. Visualizing incoherent quantum jumps as random walks on a directed graph in Hilbert space \mathcal{H} . G is the subspace of steady states that do not undergo quantum jumps. In the absence of the dashed arrow c_{μ^*} , the set of three states \mathcal{S} is closed under quantum jump, allowing a mixed steady state to form. The presence of c_{μ^*} eliminates such possibility.

$\tau \ll 1/\Gamma$, the effective Liouvillian of the 5-pulse cycle can be well-approximated using the first-order Magnus expansion by $\mathcal{L}_{\text{MP}} = (\Gamma/5) \sum_i \sum_{\alpha=0}^4 \mathcal{D}[c_\alpha^{(i)}]$. Even if different choices of rotations angles and axis are used, our scheme remains operational as long as the effective jump operators $\{\bar{c}_\alpha\}$ depopulate the entire $J = 2$ manifold. We may also employ a time independent Hamiltonian $H_{\text{CW}} = \omega \sum_i S_i^y$ to continuously rotate the ensemble, leading to an effective Liouvillian

$$\mathcal{L}_{\text{CW}} = \frac{\omega}{2\pi} \int_0^{2\pi/\omega} dt \Gamma \sum_i \mathcal{D}[e^{iH_{\text{CW}}t} c_2^{(i)} e^{-iH_{\text{CW}}t}]. \quad (5)$$

In both cases, the corresponding quantum jump rates vanish if and only if the system is in $|G\rangle$.

Uniqueness.— While our construction of \mathcal{L}_{MP} and \mathcal{L}_{CW} ensures that $|G\rangle$ is a steady state, it does not guarantee its uniqueness; for instance, one can imagine a mixed steady state that is in dynamical equilibrium due to the combination of coherent evolution and incoherent quantum jumps (Fig. 1). Such mixed steady states may arise only if there is a subspace \mathcal{S} that is orthogonal to $|G\rangle$ and closed under jump operators, $c_\mu \mathcal{S} \subseteq \mathcal{S}$ [10]. Physically, it means that the states in \mathcal{S} cannot reach $|G\rangle$ even with arbitrarily many applications of jump operators, allowing an equilibrium to form by their mixtures. In our scheme, the uniqueness is guaranteed by the following Lemma:

Lemma. *For any finite system with size $n \geq 2$ under open boundary condition, and $n \geq 4$ under periodic boundary condition, all states can reach $|G\rangle$ with some application of jump operators in \mathcal{L}_{MP} or \mathcal{L}_{CW} , implying that $|G\rangle$ is the unique steady state.*

We will now prove this Lemma for open boundary condition, where the four $|G_{ab}\rangle$ states are unique steady states; the proof for periodic boundary condition can be found in [28]. We use induction on the system size n . For $n = 2$, the uniqueness can be trivially checked by exact calculations. Now, for the sake of contradiction, let us assume that there is a subspace \mathcal{S} in a system of size $n + 1$, supporting a mixed steady state $\rho_{\mathcal{S}}$. We will show that $\rho_{\mathcal{S}}$ can reach at least one of the four $|G_{ab}\rangle$ by jump

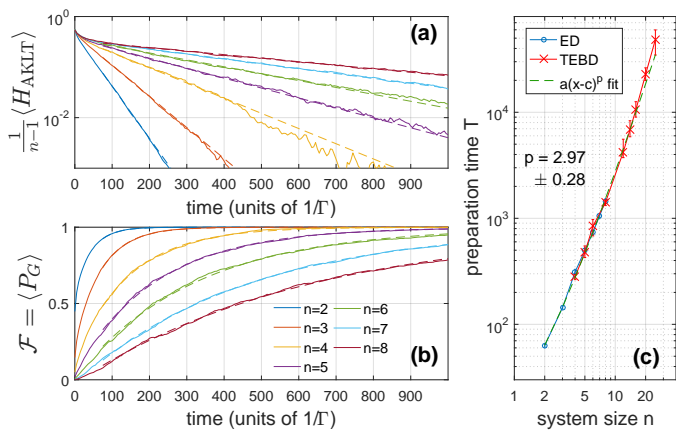


FIG. 2. (a)(b) Numerical simulation of \mathcal{L}_{MP} for $\Gamma = 1$ with maximally mixed initial state, using exact diagonalization (ED) for system sizes up to $n = 8$. The data in the long time regime are fitted to an exponential function (dashed lines). (c) Fitted preparation time to achieve $\mathcal{F} = 0.9$ from simulations using ED and TEBD algorithms, as a function of system size n , up to $n = 25$. Error bars are 90% confidence intervals.

operators in \mathcal{L}_{MP} , leading to a contradiction. (The same argument holds for \mathcal{L}_{CW} .) First, consider the following infinite time evolution $\rho_\infty \equiv \lim_{t \rightarrow \infty} \exp(t\mathcal{L}_{\text{MP}}^{[n]})\rho_S$, where $\mathcal{L}_{\text{MP}}^{[n]}$ is the Liouvillian of our protocol acting only on the first n particles. On one hand, from the inductive assumption, the first n particles must be in one of the AKLT states, implying ρ_∞ is a mixture of quantum states of the form $|\psi\rangle = \sum_{abs} \psi_{abs} |G_{ab}^n\rangle |s\rangle$, where $|G_{ab}^n\rangle$ are the ground states for n particles and the index s runs over the basis states of the $(n+1)$ -th particle. On the other hand, since \mathcal{S} is by assumption closed under jump operators, $|\psi\rangle$ must also be in \mathcal{S} and hence orthogonal to $|G_{cd}^{n+1}\rangle$. Hence, we have the following set of linear equations for ψ_{abs} :

$$\sum_{abs} \psi_{abs} \langle G_{cd}^{n+1} | f_\mu^{(n)} (|G_{ab}^n\rangle |s\rangle) = 0, \quad \forall c, d, \mu \quad (6)$$

where $f_\mu = \bar{c}_\mu$ for $\mu \in \{0, \dots, 4\}$ and $f_5 = \mathbb{1}$. Since $|G_{ab}^n\rangle$ and $|G_{cd}^{n+1}\rangle$ are exactly known, one can analytically compute these expressions and find only the trivial solution $\psi_{abs} = 0$ [28]. This implies either \mathcal{S} is not orthogonal to $|G\rangle$, or ρ_S can reach the ground state, contradicting our assumptions.

This proof naturally suggests a method to prepare an AKLT state with specified edge states instead of just a mixture of the four under open boundary condition. For instance, $|G_{\uparrow\uparrow}\rangle$ can be deterministically prepared by the addition of two jump operators, $c_L = |0\rangle\langle -|_1$ on the left edge and $c_R = |0\rangle\langle +|_n$ on the right. In this case, any linear combination of four ground states further decays into $|G_{\uparrow\uparrow}\rangle$, which is now the unique steady state.

Numerical simulations.— We now explore the efficiency of our protocol via numerical simulations. The

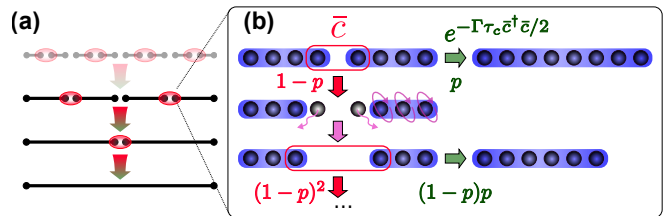


FIG. 3. (a) Scheme for preparing AKLT states in parallel to achieve logarithmic scaling. (b) Illustration of connection algorithm, where success occurs with finite probability p , while failure can be corrected with constant overhead.

simulations are performed with stochastic wavefunction method for systems of up to $n = 25$ particles, using both exact diagonalization ($n \leq 8$) and time-evolving block decimation (TEBD) algorithm [29] in MPS representations ($n \leq 25$). We initialize the system into a random product state (representing maximally mixed state), and evolve under \mathcal{L}_{MP} with open boundary condition. We then monitor the expectation value of the energy density with respect to H_{AKLT} , as well as fidelity of state preparation $\mathcal{F} = \langle P_G \rangle$, where P_G is the projector onto desired ground states. The results in Fig. 2 (a), (b) demonstrate that both observables exponentially converge to their corresponding values for AKLT states in all system sizes. We extract the state-preparation time T by first fitting $1 - \mathcal{F}$ to an exponential in the asymptotic regime and extrapolating $\mathcal{F}(T) = 0.9$. We find that T depends on the system size n , generally increasing with the number of particles. Plotted as a function of n [Fig. 2(c)], we find a polynomial scaling $T \sim \mathcal{O}(n^{2.97})$, which is consistent with previous predictions [11].

Improved scaling via parallel preparation.— We now show that the scaling can be further improved to $\mathcal{O}(\log^2 n)$. Similar to the approach used in quantum repeaters [30], this exponential speedup is possible by preparing multiple chains in parallel, which are subsequently connected into a single, long chain [Fig. 3(a)].

The key ingredient is the ability to efficiently connect or fuse two AKLT chains into a single entangled state. This is achieved with the algorithm illustrated in Fig. 3(b). First, we independently prepare two length- m chains in AKLT states, $|\psi_0\rangle = |G_{ab}^m\rangle |G_{cd}^m\rangle$. Then we turn on only the jump operators $\{\bar{c}_\alpha^{(m)}\}$ acting on the two particles $m, m+1$ at the interface, evolving for some time τ_c . Lastly, we monitor quantum jump events to determine if we have succeeded in creating an AKLT state $|\psi_f\rangle = |G_{ad}^{2m}\rangle$ with doubled length; a successful connection is heralded by the absence of quantum jumps, in which case the time evolution under non-Hermitian Hamiltonian guides the system into the AKLT states of the combined chain. For sufficiently long τ_c , the success probability is given by the overlap between initial and target states $p \simeq |\langle \psi_f | \psi_0 \rangle|^2$. On average $p \simeq 1/4$ for random edge states, but it can be maximized to $1/2$ when

$b = c$, i.e. when the two chains share the same edge states at the interface [28]. The resultant state has an exponentially small error $\epsilon \leq e^{-\mathcal{O}(\tau_c)}$. The failure of the connection is signaled by detection of a quantum jump, after which the state of the particle pair at the interface is affected through $|\psi_0\rangle \mapsto \vec{c}_\alpha^{(m)} |\psi_0\rangle$. In this case, one discards the pair of edge spins and attempts the connection procedure with chains of length $m-1$. Interestingly, in such instances we can ensure that the next attempt succeeds with the maximum probability of $p \simeq 1/2$ by performing a global rotation $U = (e^{i\pi S^y})^{\otimes m-1}$ on one of the chains [28]. This quantum feedback makes the procedure very efficient, since multiple repeated failures are exponentially unlikely, leading to an average loss of $2(1-p)/p$ particles for each connection procedure.

The analysis of the scaling shows an exponential improvement. To prepare a chain length of n , we nest the above connection algorithm in a binary tree of $\mathcal{O}(\log_2 n)$ levels; in the ℓ -th level, the average length of each chain is approximately doubled $n_\ell \simeq 2n_{\ell-1} - 2(1-p)/p$. On average, the cumulative time to reach the ℓ -th level is $T_\ell \simeq T_{\ell-1} + \tau_c/p + \tau_r(1-p)/p$, where τ_r is the time necessary to reset the edge states in each connection procedure. Provided that at the initial level $\ell = 0$, the lengths of chains $n_0 > n_c = 2(1-p)/p$, then the average time to prepare a chain of length n is $T(n) = T_0 + [(\tau_c + \tau_r(1-p))/p] \log_2[(n - n_c)/(n_0 - n_c)]$, where T_0 is the preparation time of the length n_0 chains. Since there are approximately n/n_0 connections, the final error is $\mathcal{E} \leq n\epsilon/n_0 \leq (n/n_0)e^{-\mathcal{O}(\tau_c)}$, which means we should choose $\tau_c = \mathcal{O}(\ln(n/n_0\mathcal{E}))$ to achieve a final error of \mathcal{E} . Hence, the average time necessary to prepare an AKLT state of length n with bounded error in this parallelized protocol is $T(n) \sim \mathcal{O}(\log^2 n)$. We note that imperfect detections of quantum jumps do not significantly affect the scaling of our protocol, and can be largely accounted by modifying the effective success probability p [28].

Experimental realization.— The key task in the implementation of our protocol is to engineer the nearest-neighbor jump operators. Such engineering has been previously demonstrated in systems of trapped ions [13]. Here, we provide an explicit method to realize our scheme in systems of trapped atoms [23–25] based on the Rydberg-EIT mechanism [26]. We consider a five-level system that consists of a meta-stable Rydberg state $|r\rangle$, a short-lived excited state $|e\rangle$, and three long-lived hyperfine ground states $|\pm\rangle$ and $|0\rangle$ as shown in Fig. 4(a). Using lasers, one of the ground states $|+\rangle$ is coherently coupled to the excited state with a time-dependent Rabi frequency $g(t)$. The excited state is further coupled to the Rydberg state with Rabi frequency Ω . Owing to large dipole moments, simultaneous excitations of two Rydberg states with distance R are suppressed by interaction energy shift that decays as $1/R^6$ [31].

In the absence of interactions, our coherent driving ensures that every atom supports three stable states $|-\rangle$,

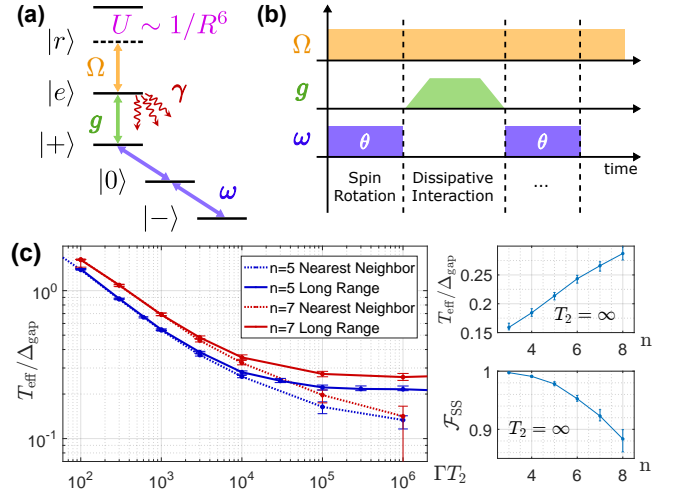


FIG. 4. (a) Atomic level diagrams for Rydberg-EIT implementation of our jump operators, where $|r\rangle$ is a Rydberg level with strong blockade interaction, and $|e\rangle$ is an excited state with short lifetime $1/\gamma$. The lower three levels encode the spin-1. (b) Pulse sequence to engineer \mathcal{L}_{MP} . (c) Effect of finite dephasing time (T_2) of spin-1 levels and long-range interaction. We use steady state fidelity \mathcal{F}_{SS} from numerical simulations to calculate effect temperature T_{eff} in units of Δ_{gap} , the energy gap of H_{AKLT} .

$|0\rangle$, and $|D(t)\rangle \propto \Omega |+\rangle - g(t) |r\rangle$ for arbitrary choices of g and Ω . We use these three states to encode the spin-1 degree of freedom. When $g(t)$ slowly increases starting from zero, $|+\rangle = |D(t=0)\rangle$ adiabatically follows $|D(t)\rangle$ without populating any excited states [see Fig. 4(b)]. In the presence of strong interactions, however, population in Rydberg state of one atom prevents another Rydberg excitation in its vicinity. Thus, as one gradually turns on $g(t)$, any neighboring pairs that are initially in $|++\rangle$ necessarily populate the excited states, followed by their decay into one of the three ground states [32]. When $0 < g \ll \Omega$, this dissipative dynamics gives rise to effective jump operators of the form $c_\phi = |\phi\rangle \langle DD|$ with a total rate

$$\Gamma_{DD} \approx -2\text{Im} \left[\frac{g^4}{\Omega^4} \frac{U}{1 + i\chi U} \right], \quad (7)$$

where $\chi \approx 1/\gamma + \gamma/(4\Omega^2)$ and ϕ is one of 9 different combinations of two-particle ground states [28, 33]. To engineer the full Liouvillian, we apply microwave pulses to the three ground states and globally rotate the spin-1 particles by $\theta \approx 2\pi/5$ [Fig. 4(b)]. When dissipative interactions and global rotations are alternated, this protocol effectively realizes a dynamics similar to \mathcal{L}_{MP} and deterministically prepares the AKLT state. We note that the experimental platform with rearrangeable atom array in Ref. [23–25] is well-suited to parallelize the implementation and exponentially shorten preparation times for large system sizes.

In a typical experiment, unwanted dissipations or interactions can affect the fidelity of our protocol by per-

turbing the steady state of dissipative dynamics. There are two main imperfections in our proposed implementation: i) the atomic states have finite dephasing time T_2 , and ii) the long-range Rydberg interaction can lead to dissipative coupling with particles beyond nearest neighbors. For the latter, we find that pairs of particles separated by distance R with interaction $U \sim 1/R^6$ acquire decay rates $\Gamma_{DD}(R) \sim 1/R^{12}$. We study the effect of these imperfections by numerical simulations of long-range effective Hamiltonian and stochastic quantum jumps that now include dephasing operators $|s\rangle\langle s|$ for $s = +, 0, -$. In order to quantify the perturbation on the steady state, we introduce an effective temperature T_{eff} defined by $\text{tr}[P_G \rho(T_{\text{eff}})] = \mathcal{F}_{\text{SS}}$, where \mathcal{F}_{SS} is the steady state fidelity and $\rho(T_{\text{eff}})$ is the thermal ensemble of H_{AKLT} at temperature T_{eff} . The results in Fig. 4(c) show that the temperature decreases with increasing dephasing time T_2 and eventually saturates due to long-range interactions. While T_{eff} also depends on system size n , we find that it stays below the gap Δ_{gap} of H_{AKLT} for all n studied in present work (up to 8). We note that the effects of long-range interaction is mitigated in our parallelized protocol, where the jump operators are turned on only for a few spin pairs that are well-separated by the length of connected chains. Also, over the course of the protocol, the effective temperature does not increase because our connection procedure ensures that $1 - \mathcal{F}$ scales linearly in system sizes while the density of excited states grows at least as fast [28].

Generalization and outlook.— Our approach can be generalized to a broader class of matrix product states. Let us consider a translation-invariant MPS with internal symmetry \mathcal{G} , which includes ground states of SPT phases [2, 34]. Our goal is to find a minimal number k_{min} of jump operators $\{c_1, c_2, \dots, c_{k_{\text{min}}}\}$ acting on neighboring pairs of particles that deterministically prepare the ground state(s) of the MPS parent Hamiltonian, assuming global symmetry operations are available. In [28], we derive a lower bound for k_{min} based on irreducible representations of the symmetry group \mathcal{G} , and provide an explicit method to construct a minimal set of jump operators saturating the bound. Given such a set $\{c_\mu\}$, the uniqueness of steady states can be explicitly checked via inductive proof using Eq. (6), which is exactly computable by diagonalizing the transfer matrix of the MPS. We note that for the purpose of preparing a ground state of SPT phase, the symmetry \mathcal{G} of a parent Hamiltonian may be larger than the symmetry $\mathcal{G}' \subset \mathcal{G}$ that protects the topological order. For example, in the case of AKLT states, $\mathcal{G} = \text{SO}(3)$ while $\mathcal{G}' = \text{D}_2$ [20].

Our parallelized protocol can also be extended to the more general case of translation-invariant MPS with symmetry. For injective MPS [1], the success probability of each connection is roughly $p \simeq 1/D^2$ or $1/D$ for random or aligned edge configurations, where D is the bond dimension of the MPS (e.g. $D = 2$ for AKLT states) [28].

The scaling of preparation time remains $\mathcal{O}(\log^2 n)$, exponentially outperforming existing dissipative protocols that do not involve parallelization and feedback [11].

Finally, we note that it may be possible to generalize our symmetry-based dissipative preparation scheme to higher dimensional many-body entangled states. Many such states are described by Projected Entangled Pair States (PEPS), a natural generalization of MPS for arbitrary lattices, which also allow construction of frustration-free parent Hamiltonians [35] to be converted into jump operators. However, our inductive uniqueness proof does not extend straightforwardly, since exact computation of expectation values of a generic PEPS is intractable [36]. Further investigations are thus necessary to extend our strategy to higher dimensions, which can support even more interesting, long-range entangled states.

We thank H. Pichler and F. Reiter for useful discussion. This work was supported through NSF, CUA, Vannevar Bush Faculty Fellowship, AFOSR MURI, and Moore Foundation. L.Z. is supported by NSF Graduate Research Fellowship under Grant No. DGE1144152. S.C. is supported by Kwanjeong Educational Foundation.

* These authors contributed equally to this work.

- [1] D. Perez-Garcia, F. Verstraete, M. M. Wolf, and J. I. Cirac, *Quantum Inf. Comput.* **7**, 401 (2007).
- [2] N. Schuch, D. Pérez-García, and I. Cirac, *Phys. Rev. B* **84**, 165139 (2011).
- [3] I. Cohen, P. Richerme, Z.-X. Gong, C. Monroe, and A. Retzker, *Phys. Rev. A* **92**, 012334 (2015).
- [4] J. G. Bohnet, B. C. Sawyer, J. W. Britton, M. L. Wall, A. M. Rey, M. Foss-Feig, and J. J. Bollinger, *Science* **352**, 1297 (2016).
- [5] R. M. W. van Bijnen and T. Pohl, *Phys. Rev. Lett.* **114**, 243002 (2015).
- [6] A. Mazurenko, C. S. Chiu, G. Ji, M. F. Parsons, M. Kanász-Nagy, R. Schmidt, F. Grusdt, E. Demler, D. Greif, and M. Greiner, *Nature (London)* **545**, 462 (2017).
- [7] J. Cai, A. Retzker, F. Jelezko, and M. B. Plenio, *Nat. Phys.* **9**, 168 (2013).
- [8] B. Yan, S. A. Moses, B. Gadway, J. P. Covey, K. R. A. Hazzard, A. M. Rey, D. S. Jin, and J. Ye, *Nature (London)* **501**, 521 (2013).
- [9] R. Barends *et al.*, *Nature (London)* **534**, 222 (2016).
- [10] B. Kraus, H. P. Büchler, S. Diehl, A. Kantian, A. Micheli, and P. Zoller, *Phys. Rev. A* **78**, 042307 (2008).
- [11] F. Verstraete, M. M. Wolf, and J. I. Cirac, *Nat. Phys.* **5**, 633 (2009).
- [12] J. Cho, S. Bose, and M. S. Kim, *Phys. Rev. Lett.* **106**, 020504 (2011).
- [13] J. T. Barreiro, M. Mller, P. Schindler, D. Nigg, T. Monz, M. Chwalla, M. Hennrich, C. F. Roos, P. Zoller, and R. Blatt, *Nature (London)* **470**, 486 (2010).
- [14] M. J. Kastoryano, F. Reiter, and A. S. Sørensen, *Phys. Rev. Lett.* **106**, 090502 (2011).

- [15] F. Reiter, L. Tornberg, G. Johansson, and A. S. Sørensen, *Phys. Rev. A* **88**, 032317 (2013).
- [16] D. D. B. Rao and K. Mølmer, *Phys. Rev. A* **90**, 062319 (2014).
- [17] M. Roghani and H. Weimer, arXiv:1611.09612.
- [18] I. Affleck, T. Kennedy, E. H. Lieb, and H. Tasaki, *Phys. Rev. Lett.* **59**, 799 (1987).
- [19] F. Haldane, *Phys. Lett. A* **93**, 464 (1983).
- [20] F. Pollmann, A. M. Turner, E. Berg, and M. Oshikawa, *Phys. Rev. B* **81**, 064439 (2010).
- [21] M. den Nijs and K. Rommelse, *Phys. Rev. B* **40**, 4709 (1989).
- [22] D. Pérez-García, M. M. Wolf, M. Sanz, F. Verstraete, and J. I. Cirac, *Phys. Rev. Lett.* **100**, 167202 (2008).
- [23] M. Endres, H. Bernien, A. Keesling, H. Levine, E. R. Anschuetz, A. Krajenbrink, C. Senko, V. Vuletic, M. Greiner, and M. D. Lukin, *Science* **354**, 1024 (2016).
- [24] D. Barredo, S. de Léséleuc, V. Lienhard, T. Lahaye, and A. Browaeys, *Science* **354**, 1021 (2016).
- [25] B. J. Lester, N. Luick, A. M. Kaufman, C. M. Reynolds, and C. A. Regal, *Phys. Rev. Lett.* **115**, 073003 (2015).
- [26] D. Petrosyan, J. Otterbach, and M. Fleischhauer, *Phys. Rev. Lett.* **107**, 213601 (2011).
- [27] C. Gardiner and P. Zoller, *Quantum Noise: A Handbook of Markovian and Non-Markovian Quantum Stochastic Methods with Applications to Quantum Optics*, Vol. 56 (Springer Science & Business Media, 2004).
- [28] Please see Supplemental Material online.
- [29] G. Vidal, *Phys. Rev. Lett.* **91**, 147902 (2003).
- [30] H.-J. Briegel, W. Dür, J. I. Cirac, and P. Zoller, *Phys. Rev. Lett.* **81**, 5932 (1998).
- [31] M. D. Lukin, M. Fleischhauer, R. Cote, L. M. Duan, D. Jaksch, J. I. Cirac, and P. Zoller, *Phys. Rev. Lett.* **87**, 037901 (2001).
- [32] In practice, the excited state can also decay into other hyperfine ground states, which can then be repumped to the excited state using additional lasers.
- [33] F. Reiter and A. S. Sørensen, *Phys. Rev. A* **85**, 032111 (2012).
- [34] M. Sanz, M. M. Wolf, D. Pérez-García, and J. I. Cirac, *Phys. Rev. A* **79**, 042308 (2009).
- [35] D. Perez-Garcia, F. Verstraete, M. M. Wolf, and J. I. Cirac, *Quantum Inf. Comput.* **8**, 650 (2008).
- [36] N. Schuch, M. M. Wolf, F. Verstraete, and J. I. Cirac, *Phys. Rev. Lett.* **98**, 140506 (2007).

Supplementary Material for “Symmetry-protected dissipative preparation of a matrix product state”

Leo Zhou,* Soonwon Choi,* and Mikhail D. Lukin
Department of Physics, Harvard University, Cambridge, Massachusetts 02138, USA
 (Dated: June 8, 2017)

CONTENTS

I.	Matrix product state representation of AKLT states	1
II.	Effective Liouvillian	2
III.	Uniqueness of steady states	2
	A. Open Boundary Condition	3
	B. Periodic Boundary Condition	3
IV.	Detailed analysis of Rydberg-EIT implementation proposal	4
V.	Detailed analysis of parallelized protocol	5
	A. Non-Hermitian time evolution	5
	B. Success probability of connection	5
	C. Effect of imperfect quantum jump detection	6
	D. Scaling of imperfection in Rydberg-EIT implementation	8
VI.	Generalization	9
	A. Notations and useful properties of matrix product states	9
	B. Internal Symmetries of MPS	10
	C. Generalization of our protocol	11
	D. Parallelized protocol for general case	12
	References	14

I. MATRIX PRODUCT STATE REPRESENTATION OF AKLT STATES

The ground states of AKLT Hamiltonian can be exactly represented by matrix product states (MPS). More specifically, for a system of n spin-1 particles, the AKLT ground states can be written as

$$|G_{ab}\rangle = |A_{ab}^n\rangle = \sum_{\{s_i\}} \langle a | A^{(s_1)} A^{(s_2)} \dots A^{(s_n)} | b \rangle |s_1 s_2 \dots s_n\rangle, \quad (1)$$

where $s_i \in \{|m_z = \pm 1\rangle, |m_z = 0\rangle\}$ runs over three spin projections of particles at site i , and $a, b \in \{\uparrow, \downarrow\}$ specify the edge states of $|G_{ab}\rangle$. Here and below, the notation $|A_{ab}^n\rangle$ indicates translational-invariant MPS of n particles with open boundary condition specified by a and b , and $|A^n\rangle$ denotes the state with periodic boundary condition, i.e. $|A^n\rangle = \sum_a |A_{aa}^n\rangle$. In this way, one can conveniently rewrite the quantum state of an n -particle system as a linear superposition of composite systems, each with m and $n - m$ particles, i.e. $|A_{ab}^n\rangle = \sum_c |A_{ac}^m\rangle |A_{cb}^{n-m}\rangle$. In the canonical form [1], the explicit MPS representation of AKLT states is given by

$$A^{(+)} = \sqrt{\frac{2}{3}}\sigma^+, \quad A^{(0)} = -\sqrt{\frac{1}{3}}\sigma^z, \quad A^{(-)} = -\sqrt{\frac{2}{3}}\sigma^-. \quad (2)$$

* These authors contributed equally to this work.

In this representation, the many-body overlap between two AKLT states with different boundary conditions can be straightforwardly computed. More explicitly, using the transfer matrix [1], we obtain

$$\langle A_{ab}^n | A_{a'b'}^n \rangle = \langle ab | \begin{pmatrix} \frac{1}{2}(1 + \epsilon^n) & 0 & 0 & \epsilon^n \\ 0 & \frac{1}{2}(1 - \epsilon^n) & 0 & 0 \\ 0 & 0 & \frac{1}{2}(1 - \epsilon^n) & 0 \\ \epsilon^n & 0 & 0 & \frac{1}{2}(1 + \epsilon^n) \end{pmatrix} | a'b' \rangle, \quad (3)$$

where $|ab\rangle, |a'b'\rangle \in \{\uparrow\uparrow, \uparrow\downarrow, \downarrow\uparrow, \downarrow\downarrow\}$ and $\epsilon \equiv -1/3$. We note that this MPS is injective (see section VI A and Ref. [1]).

II. EFFECTIVE LIOUVILLIAN

Our proposal for preparing AKLT states uses only one type of jump operator, e.g. $c = |00\rangle\langle ++|$. The dissipative dynamics due to this jump operator is $\mathcal{L}_0 = \Gamma \sum_i \mathcal{D}[c^{(i)}]$, where i enumerates the pair of neighboring sites $(i, i+1)$. Our key idea is to use coherent global manipulations, corresponding to operations in the symmetry group, so as to effectively realize additional jump operators. This can be achieved either by periodically applying pulsed global spin rotations (symmetry operations), or by continuously rotating the spins.

In the first, multi-pulse sequence approach, we apply pulses $V_\theta = (e^{i\theta S_y})^{\otimes n}$, separated by interval of τ each. Then in the rotating frame, we have the time-dependent Liouvillian:

$$\mathcal{L}_{\text{MP}}(t) = (V_\theta^\dagger)^k \mathcal{L}_0 V_\theta^k \quad \text{for } k\tau \leq t < (k+1)\tau. \quad (4)$$

Suppose we choose $\theta = 2\pi/\ell$ for some integer ℓ , then this dynamics is periodic with period $\ell\tau$, since $V_{2\pi/\ell}^\ell = 1$. In the limit of fast pulses $\tau \ll 1/\Gamma$, we can use the first-order Magnus expansion to derive a simpler, effective time-independent Liouvillian that approximate the dynamics:

$$\bar{\mathcal{L}}_{\text{MP}} = \frac{1}{\ell\tau} \int_0^{\ell\tau} \mathcal{L}_{\text{MP}}(t) dt = \frac{\Gamma}{\ell} \sum_i \sum_{\alpha=0}^{\ell-1} \mathcal{D}[\bar{c}_\alpha^{(i)}], \quad (5)$$

where $\bar{c}_\alpha = (V_{2\pi/\ell}^\dagger)^\alpha c V_{2\pi/\ell}^\alpha$.

Alternatively, we may employ a continuous wave approach by introducing a time-independent Hamiltonian $H_{\text{CW}} = \omega \sum_i S_i^y$. Then in the rotating frame, we have $c(t) = e^{i\omega t S_y} c e^{-i\omega t S_y}$, and

$$\dot{\rho} = \mathcal{L}_{\text{CW}}(t)\rho \equiv \Gamma \sum_i \mathcal{D}[c^{(i)}(t)]\rho. \quad (6)$$

In this frame, the dynamics is periodic with period $2\pi/\omega$. Again, we compute the effective time-independent Liouvillian

$$\bar{\mathcal{L}}_{\text{CW}} = \frac{\omega}{2\pi} \int_0^{2\pi/\omega} \mathcal{L}_{\text{CW}}(t) dt = \sum_i \sum_{\beta=0}^{\ell-1} \Gamma_\beta \mathcal{D}[\bar{c}_\beta^{(i)}], \quad (7)$$

obtained by time-averaging (first-order Magnus expansion) as an approximation. The effective jump operator \bar{c}_β in the standard form of Liouvillian can be obtained by diagonalizing the superoperator acting on the space of density operator. More explicitly, we diagonalize a Hermitian matrix $L = U^\dagger \Lambda U$, whose entries $L_{ii',jj'}$ are given by

$$L_{ii',jj'} \equiv \left\langle ij \left| \frac{\omega}{2\pi} \int_0^{2\pi/\omega} dt \Gamma c^*(t) \otimes c(t) \right| i'j' \right\rangle = \sum_\beta U_{\beta,ii'}^* \Lambda_\beta U_{\beta,jj'} \equiv \left\langle ij \left| \sum_\beta \Gamma_\beta \bar{c}_\beta^* \otimes \bar{c}_\beta \right| i'j' \right\rangle. \quad (8)$$

We can read off $\Gamma_\beta = \Lambda_\beta$, and $\bar{c}_\beta = \sum_{k,k'} U_{\beta,kk'} |k\rangle\langle k'|$. For our example choice of $c(t=0) = |00\rangle\langle ++|$, we obtain $\ell = 9$ independent jump operator after evaluating the integral and diagonalizing, each with rate $\Gamma_\beta/\Gamma = 7/32, 3/16, 3/16, 1/8, 1/8, 1/16, 1/16, 1/64, 1/64$.

III. UNIQUENESS OF STEADY STATES

In this section, we provide detailed proofs that our proposed $\bar{\mathcal{L}}_{\text{MP}}$ and $\bar{\mathcal{L}}_{\text{CW}}$ have the AKLT states as unique steady states, for $n \geq 2$ under open boundary condition, and $n \geq 4$ under periodic boundary condition.

A. Open Boundary Condition

Although the proof for open boundary condition has been sketched in the main text, here we provide more detailed analysis. We prove by induction. Let us denote $\mathcal{L}_i = \sum_{\alpha=0}^{\ell-1} \Gamma_{\alpha} \mathcal{D}[\bar{c}_{\alpha}^{(i)}]$ as the Liouvillian acting only on sites i and $i+1$, and $\mathcal{L}_{[n]} = \sum_{i=1}^{n-1} \mathcal{L}_i$. The base case of $n=2$ can easily be checked numerically or by exact calculations. The inductive hypothesis is that $\mathcal{L}_{[n]}$ only has the AKLT states $|A_{ab}^n\rangle$ as steady states. Assume for the sake of contradiction that there exist other steady states for $\mathcal{L}_{[n+1]}$ on $n+1$ particles. This means that there exists a subspace \mathcal{S} where $c_{\alpha}^{(i)} \mathcal{S} \subseteq \mathcal{S}$ for any i and α , and $\mathcal{S} \perp G \equiv \text{span}\{|A_{ab}^{n+1}\rangle\}$ [2]. This assumption implies that $f(\{\bar{c}_{\alpha}^{(i)}\})|\psi\rangle \in \mathcal{S}$ for any $|\psi\rangle \in \mathcal{S}$ and any polynomial $f(\cdot)$ of the jump operators. Now, let $\rho_{\mathcal{S}}$ be a steady state supported by \mathcal{S} , so that $\text{range}(\rho_{\mathcal{S}}) \subseteq \mathcal{S}$. Then let us perform the infinite time evolution $\rho_{\infty} = \lim_{t \rightarrow \infty} \exp(\mathcal{L}_{[n]}t)\rho_{\mathcal{S}}$, which is a steady state of $\mathcal{L}_{[n]}$. Consider any state $|\psi\rangle \in \text{range}(\rho_{\infty})$.

On one hand, by our inductive hypothesis, any steady state of $\mathcal{L}_{[n]}$ must look like one of the AKLT states on the first n particles. Hence, we can write $|\psi\rangle = \sum_{abs} \psi_{abs} |A_{ab}^n\rangle |s\rangle$, where $s \in \{+, 0, -\}$. On the other hand, we must have $|\psi\rangle \in \mathcal{S}$ since $\mathcal{L}_{[n]}$ contains the same jump operators found in $\mathcal{L}_{[n+1]}$ that leave \mathcal{S} invariant by assumption. Let us denote $f_{\mu} = \bar{c}_{\mu}$ for $\mu = 0, \dots, \ell-1$, and $f_{\mu} = \mathbf{1}$ for $\mu = \ell$. By the assumption that $f_{\mu}^{(n)}|\psi\rangle \in \mathcal{S} \perp G$, we require that for any $p, q \in \{\uparrow, \downarrow\}$ and $0 \leq \mu \leq \ell$, the following set of linear equations for ψ_{abs} must be true:

$$\begin{aligned} 0 &= \langle A_{pq}^{n+1} | f_{\mu}^{(n)} | \psi \rangle = \sum_{abs} \psi_{abs} \langle A_{pq}^{n+1} | f_{\mu}^{(n)} (|A_{ab}^n\rangle |s\rangle) = \sum_{abcrs} \psi_{abs} \langle A_{pr}^{n-1} | A_{ac}^{n-1} \rangle \times \langle A_{rq}^2 | f_{\mu} | A_{cb}^1 \rangle |s\rangle \\ &= \sum_{abs} B_{pq\mu}^{abs} \psi_{abs} \equiv \mathbf{B} \vec{\psi}, \end{aligned} \quad (9)$$

where $\vec{\psi}$ is a 12-dimensional vector and \mathbf{B} is a $4(\ell+1)$ -by-12 matrix. The matrix elements of \mathbf{B} given by $B_{pq\mu}^{abs} = \sum_{cr} \langle A_{pr}^{n-2} | A_{ac}^{n-2} \rangle \times \langle A_{rq}^2 | f_{\mu} | A_{cb}^1 \rangle |s\rangle$ can be calculated analytically, since the first factor comes from diagonalizing the transfer matrix, and the second factor is computed in a small 9-dimensional Hilbert space. Now if $\det(\mathbf{B}^{\dagger} \mathbf{B}) \neq 0$, then the matrix \mathbf{B} has full rank, indicating that we only have the trivial solution $\psi_{abs} = 0$. Then, by contradiction, \mathcal{S} cannot exist, and $|A_{ab}^{n+1}\rangle$ are the unique steady states of $\mathcal{L}_{[n+1]}$.

Therefore, it only remains to compute $\det(\mathbf{B}^{\dagger} \mathbf{B})$ for \mathcal{L} in our proposals. Let us first consider $\bar{\mathcal{L}}_{\text{MP}}$, with $\ell = 5$ corresponding to rotation pulses with $\theta = 2\pi/5$. For this, we explicitly find

$$\det(\mathbf{B}^{\dagger} \mathbf{B}) = \frac{5^8 (x+3)^6 (x-1)^2 (3x+1)^6 (x^2+27)^2 (x^2-6x+45)^3}{2^{40} 9^{13} x^{24}}, \quad x \equiv (-3)^n. \quad (10)$$

It's easy to see that this is only zero for $n = 0, \pm 1$, so our inductive proof holds for $n \geq 2$. For $\bar{\mathcal{L}}_{\text{CW}}$, which has $\ell = 9$, we find

$$\det(\mathbf{B}^{\dagger} \mathbf{B}) = \frac{13(x+3)^6 (x-1)^2 (3x+1)^6 (5x^2-6x+153)^2 (13x^2-66x+549)(65x^2-342x+2781)^2}{2^{20} 7^4 9^{17} x^{24}}, \quad (11)$$

where we again denote $x \equiv (-3)^n$. This is also only nonzero when $n = 0, \pm 1$, proving that the steady states of $\bar{\mathcal{L}}_{\text{MP}}$ and $\bar{\mathcal{L}}_{\text{CW}}$ are unique for $n \geq 2$.

B. Periodic Boundary Condition

The uniqueness proof for periodic boundary condition builds on the result for open boundary condition, and is very similar in spirit. Let the Liouvillian under periodic boundary condition be $\mathcal{L}_{[n]}^{\circ} = \mathcal{L}_{[n]} + \mathcal{L}_{n,1}$, where $\mathcal{L}_{n,1} = \sum_{\alpha=0}^{\ell-1} \Gamma_{\alpha} \mathcal{D}[\bar{c}_{\alpha}^{(n,1)}]$ acts on sites n and 1 . Assume for the sake of contradiction that there exists a steady state of $\mathcal{L}_{[n]}^{\circ}$ other than $|A^n\rangle = \sum_a |A_{aa}^n\rangle$, supported by a subspace $\mathcal{S} \perp |A^n\rangle$. Let $\rho_{\mathcal{S}}$ be such a steady state, on which we perform the infinite time evolution to obtain $\rho_{\infty} = \lim_{t \rightarrow \infty} \exp(\mathcal{L}_{[n]}t)\rho_{\mathcal{S}}$. Note ρ_{∞} is a steady state of $\mathcal{L}_{[n]}$. Again, consider any state $|\psi\rangle \in \text{range}(\rho_{\infty}) \subseteq \mathcal{S}$.

From our results for open boundary condition, we know that we can write $|\psi\rangle = \sum_{ab} \psi_{ab} |A_{ab}^n\rangle$. Additionally, we must have $f(\{\bar{c}_{\alpha}^{(i,i+1)}\})|\psi\rangle \in \mathcal{S}$ for any polynomial $f(\cdot)$ of jump operators. It turns out that unlike in the case of open boundary condition, polynomials of degree one are not sufficient to demonstrate uniqueness of steady states. Instead, let us consider polynomials of the form $f_{\mu}^{(n,1)} f_{\nu}^{(n-1,n)} f_{\lambda}^{(n,1)}$, where $f_{\mu} = \bar{c}_{\mu}$ for $\mu = 0, \dots, \ell-1$ and $f_{\mu} = \mathbf{1}$ for $\mu = \ell$.

Hence, we have the following set of linear equations for ψ_{ab} :

$$0 = \langle A^n | f_\mu^{(n,1)} f_\nu^{(n-1,n)} f_\lambda^{(n,1)} | \psi \rangle = \sum_{ab} \psi_{ab} \langle A^n | f_\mu^{(n,1)} f_\nu^{(n-1,n)} f_\lambda^{(n,1)} | A_{ab}^n \rangle = \sum_{ab} B_{\mu\nu\lambda}^{ab} \psi_{ab} = \mathbf{B} \vec{\psi},$$

where $B_{\mu\nu\lambda}^{ab} = \sum_{cdpqr} (\langle A_{pq}^1 | \langle A_{qr}^{n-3} | \langle A_{rp}^2 | f_\mu^{(n,1)} f_\nu^{(n-1,n)} f_\lambda^{(n,1)} (|A_{ac}^1 \rangle |A_{cd}^{n-3} \rangle |A_{db}^2 \rangle) = \sum_{cdqr} \langle A_{qr}^{n-3} | A_{cd}^{n-3} \rangle \times \langle A_{rq}^3 | (\mathbf{1} \otimes f_\mu) (f_\nu \otimes \mathbf{1}) (\mathbf{1} \otimes f_\lambda) | A_{db}^2 \rangle | A_{ac}^1 \rangle.$ (12)

Here, $\vec{\psi}$ is a 4-dimensional vector, and \mathbf{B} is a $(\ell + 1)^3$ -by-4 matrix. For $\bar{\mathcal{L}}_{\text{MP}}$ with $\ell = 5$, we find

$$\det(\mathbf{B}^\dagger \mathbf{B}) = \frac{5^9 7^3 (x+3)^2 (x+27)^6}{2^{33} 3^{15} x^8}, \quad x \equiv (-3)^n. \quad (13)$$

And similarly, for $\bar{\mathcal{L}}_{\text{CW}}$, which has $\ell = 9$, we find

$$\det(\mathbf{B}^\dagger \mathbf{B}) = \frac{5 \times 283^2 (x+3)^2 (x+27)^6}{2^{275} 3^{17} x^8}, \quad x \equiv (-3)^n. \quad (14)$$

Both of these vanishes only when $n = 1, 3$. Thus, the steady states of $\bar{\mathcal{L}}_{\text{MP}}$ and $\bar{\mathcal{L}}_{\text{CW}}$ are unique for $n \geq 4$. The fact that they vanish for $n = 3$ corroborates numerical simulations that also demonstrate the existence of undesired steady states for $n = 3$ under periodic boundary condition.

IV. DETAILED ANALYSIS OF RYDBERG-EIT IMPLEMENTATION PROPOSAL

In this section, we derive the effective dissipative interaction between two nearby particles for our Rydberg-EIT implementation scheme introduced in the main text. Consider two particles interacting via the Rydberg shift $H_{\text{int}} = U |rr\rangle \langle rr|$. Their effective (non-Hermitian) Hamiltonian under the Rydberg-EIT scheme proposed in the main text is

$$\begin{aligned} H_{\text{eff}} &= \sum_{j=1}^2 \left[(g|+\rangle \langle e| + \Omega|r\rangle \langle e| + h.c.) - i\frac{\gamma}{2}|e\rangle \langle e| \right]_j + U |rr\rangle \langle rr| \\ &= \sum_{j=1}^2 \left[\Delta(|B\rangle \langle e| + h.c.) - i\frac{\gamma}{2}|e\rangle \langle e| \right]_j + U |rr\rangle \langle rr|, \end{aligned} \quad (15)$$

where $\Delta = \sqrt{\Omega^2 + g^2}$, $|D\rangle = (\Omega|+\rangle - g|r\rangle)/\Delta$ is the EIT-dark state, and $|B\rangle = (g|+\rangle + \Omega|r\rangle)/\Delta$ a state orthogonal to $|D\rangle$ that we call EIT-bright state. Now consider a general two-particle wavefunction $|\psi\rangle = \sum_a c_{aa} |aa\rangle + \sum_{a<b} c_{ab} (|ab\rangle + |ba\rangle)/\sqrt{2}$, where we've restricted ourselves to working in the symmetric subspace. Then the equations of motion for the coefficients are

$$\begin{cases} i\dot{c}_{DD} &= \frac{g^4 U}{\Delta^4} c_{DD} - \frac{\sqrt{2} g^3 \Omega U}{\Delta^4} c_{DB} + \frac{g^2 \Omega^2 U}{\Delta^4} c_{BB} \\ i\dot{c}_{De} &= -i\frac{\gamma}{2} c_{De} + \Delta c_{DB} \\ i\dot{c}_{DB} &= \frac{2g^2 \Omega^2 U}{\Delta^4} c_{DB} + \Delta c_{De} - \frac{\sqrt{2} g^3 \Omega U}{\Delta^4} c_{DD} - \frac{\sqrt{2} g \Omega^3 U}{\Delta^4} c_{BB} \\ i\dot{c}_{ee} &= -i\gamma c_{ee} + \sqrt{2} \Delta c_{eB} \\ i\dot{c}_{eB} &= -i\frac{\gamma}{2} c_{eB} + \sqrt{2} \Delta (c_{ee} + c_{BB}) \\ i\dot{c}_{BB} &= \frac{\Omega^4 U}{\Delta^4} c_{BB} + \sqrt{2} \Delta c_{eB} - \frac{\sqrt{2} g \Omega^3 U}{\Delta^4} c_{DB} + \frac{g^2 \Omega^2 U}{\Delta^4} c_{DD} \end{cases}. \quad (16)$$

In the limit of $U \ll g, \Omega, \gamma$, or $g \ll \Omega, \gamma, U$, and assuming we start initially with $|\psi\rangle = |DD\rangle$, we can adiabatically eliminate the fast dynamics involving coefficients $\{c_{ab}\}$ other than c_{DD} . This procedure can be effectively achieved by setting $\dot{c}_{ab} = 0$ for $ab \neq DD$, allowing us to obtain

$$i\dot{c}_{DD} = U_{DD} c_{DD} \quad \text{where} \quad U_{DD} = \frac{g^4}{\Delta^4} \frac{U}{1 + i\chi U} \quad \text{and} \quad \chi = \frac{\Omega^2 (\Omega^2 + (1 + 3g^2/\Delta^2)\gamma^2/4)}{\Delta^4 \gamma}. \quad (17)$$

Here, $\text{Re}[U_{DD}]$ is the interaction-induced energy shift, and $\Gamma_{DD} = -2\text{Im}[U_{DD}]$ is the two-body effective decay rate.

A more general version of adiabatic elimination for open system can be found in Ref. [3], where effective jump operator can also be obtained. Consider original jump operators of the form $L_{s,j} = |s\rangle\langle e|_j$ with rate γ_s for $s \in \{+, 0, -\}$, $j = 1, 2$. We also set $\gamma_+ + \gamma_0 + \gamma_- = \gamma$. Then the effective jump operators are of the form

$$L_{\text{eff}}^{s,1} = |s\tilde{e}\rangle\langle DD|, \quad L_{\text{eff}}^{s,2} = |\tilde{e}s\rangle\langle DD|, \quad \text{each with rate } \frac{\gamma_s}{2\gamma}\Gamma_{DD}, \quad (18)$$

and $|\tilde{e}\rangle \propto \frac{\Omega\gamma}{2\Delta}|B\rangle - i\Omega|e\rangle - \frac{g\gamma}{\Delta}|D\rangle$. Note $|\tilde{e}\rangle$ will further decay through the original jump operator $L_{s,j}$. Assuming we are in the regime $\gamma \gg \gamma_s\Gamma_{DD}/2\gamma$ so that $|\tilde{e}\rangle$ is a short-lived intermediate state, we can approximate the overall effective dynamics with jump operators of the form $L_{\text{eff}}^{ss'} = |ss'\rangle\langle DD|$ for $s, s' \in \{+, 0, -\}$.

V. DETAILED ANALYSIS OF PARALLELIZED PROTOCOL

A. Non-Hermitian time evolution

In this section, we use the stochastic wavefunction formalism for open system dynamics. Namely, we define an effective non-Hermitian Hamiltonian $H_{\text{eff}} = H - i\sum_{\mu}\Gamma_{\mu}c_{\mu}^{\dagger}c_{\mu}/2$, where H is the hamiltonian of the system and $c^{(i)}$ are quantum jump operators. A system evolves under H_{eff} until it undergoes quantum jump $|\psi\rangle \mapsto c_{\mu}|\psi\rangle$ at a rate $\langle\psi|\Gamma_{\mu}c_{\mu}^{\dagger}c_{\mu}|\psi\rangle$. In our protocol to prepare AKLT states, $H = 0$ since we work in the rotating frame. Hence, H_{eff} is anti-Hermitian and thus diagonalizable with eigenvalues $\lambda_{\alpha} = -i\gamma_{\alpha}/2$. It is assumed that our desired states are ‘‘dark states’’, which are eigenvectors with zero imaginary part of the eigenvalue. For simplicity and illustrative purpose, let us also assume there just one dark state $|0\rangle$ with eigenvalue $\lambda_0 = 0$, and the rest of the eigenvalues are sorted by $0 < \gamma_1 \leq \gamma_2 \leq \dots$. Let us decompose the initial state in the eigenbasis $|\psi_0\rangle = \sum_{\alpha}c_{\alpha}|\alpha\rangle = c_0|0\rangle + c_1|1\rangle + \dots$. The evolution under H_{eff} yields the following unnormalized state

$$|\tilde{\psi}(t)\rangle \equiv e^{-iH_{\text{eff}}t}|\psi_0\rangle = c_0|0\rangle + c_1e^{-\gamma_1 t/2}|1\rangle + \dots \quad (19)$$

The probability of undergoing no quantum jump over a time duration T is

$$p_0(T) = \langle\tilde{\psi}(T)|\tilde{\psi}(T)\rangle = |c_0|^2 + |c_1|^2e^{-\gamma_1 T} + \dots \geq |c_0|^2 = |\langle 0|\psi_0\rangle|^2. \quad (20)$$

Conditioned on such an event, the fidelity of the quantum state preparation is

$$\mathcal{F}(T) = |\langle 0|\psi(T)\rangle|^2 = \frac{|\langle 0|\tilde{\psi}(T)\rangle|^2}{\langle\tilde{\psi}(T)|\tilde{\psi}(T)\rangle} = \frac{|c_0|^2}{|c_0|^2 + |c_1|^2e^{-\gamma_1 T} + \dots} = 1 - \mathcal{O}(e^{-\gamma_1 T}) \quad \text{if } |c_0|^2 > 0, \quad (21)$$

where we find that the fidelity exponentially approaches to unity. This allows for effective ‘‘cooling’’ of the system into the desired state when there is no quantum jump for $T \gg 1/\gamma_1$, which occurs with probability $p_0 \simeq |\langle 0|\psi_0\rangle|^2$.

B. Success probability of connection

Consider an arbitrary initial state of two unentangled length- n chains of AKLT states, $|\psi_0\rangle = \mathcal{N}_0(\sum_b\alpha_b|A_{ab}^n\rangle) \otimes (\sum_c\beta_c|A_{cd}^n\rangle)$, where $\vec{\alpha}, \vec{\beta} \in \mathbb{C}^2$ characterizes the edge states at the interface, and \mathcal{N}_0 is normalization constant. We want to cool this state into the desired state of $|\psi_f^{2n}\rangle = \mathcal{N}_f|A_{ad}^{2n}\rangle$ by turning on the jump operators acting at the interface (i.e. spin n and $n+1$). The success probability of connection is the probability of undergoing no quantum jumps for sufficiently long time, which can be computed using Eq. (3) to be

$$p \simeq |\langle\psi_f^{2n}|\psi_0\rangle|^2 = \frac{|\vec{\alpha} \cdot \vec{\beta}|^2}{2|\vec{\alpha}|^2|\vec{\beta}|^2} + \mathcal{O}(\epsilon^n), \quad \text{where } \epsilon = -1/3. \quad (22)$$

If the edge states $\vec{\alpha}, \vec{\beta}$ are random vectors in \mathbb{C}^2 , we have on average $p \simeq 1/4$. When the edge states are aligned, i.e. $\vec{\alpha} \parallel \vec{\beta}$, we obtain the maximum success probability of $p_{\text{max}} = 1/2$.

In the case of failure, it turns out that quantum jumps affect the success probability of subsequent connections, which in fact vanishes for our protocol unless we perform quantum feedback by applying a global spin rotations to one

of the chains. In our protocol, the jump operators are of the form $c_\theta = V_\theta^{\dagger\otimes 2}|\phi\rangle\langle ++|V_\theta^{\otimes 2}$, where $V_\theta = e^{i\theta S_y}$. In the event of a quantum jump c_θ , the state after discarding the two spins at the interface is $|\psi_1\rangle = \mathcal{N}_1(\sum_{b'} \tilde{\alpha}_{b'} |A_{ab'}^{n-1}\rangle) \otimes (\sum_{c'} \tilde{\beta}_{c'} |A_{c'd}^{n-1}\rangle)$, where $\tilde{\alpha}_{b'} = \sum_b \langle +|V_\theta|A_{b'b}^1\rangle \alpha_b$ and $\tilde{\beta}_{c'} = \sum_c \langle +|V_\theta|A_{c'c}^1\rangle \beta_c$. Then we find

$$\vec{\tilde{\alpha}} \cdot \vec{\tilde{\beta}} = \sum_{b'} \tilde{\alpha}_{b'} \tilde{\beta}_{b'} = \sum_{bc} \langle ++|V_\theta^{\otimes 2}|A_{cb}^2\rangle \alpha_b \beta_c = 0. \quad (23)$$

This is zero regardless of initial states α_b and β_c , due to the fact that $V_\theta^\dagger \otimes V_\theta^\dagger |++\rangle$ has total angular momentum $J = 2$ and thus zero overlap with the AKLT state $|A_{cb}^2\rangle$. Hence, the success probability of the next connection attempt is $p' \simeq |\langle \psi_f^{2n-2} | \psi_0 \rangle|^2 = \mathcal{O}(\epsilon^n)$, which vanishes for a large system size. In fact, this vanishing success probability can be traced back to the bond-inversion symmetry of AKLT states, which we discuss further in Sec. VID. Remarkably, we can restore the success probability to its maximum value p_{\max} by applying a global π -rotation $U = e^{i\pi S_y}$ to all spins in one of the two chains (same rotational axis as V_θ). In other words, we attempt the next connection on the state

$$|\psi'_1\rangle = U^{\otimes n-1} \otimes \mathbf{1}^{\otimes n-1} |\psi_1\rangle = \mathcal{N}_1 \left(\sum_{b'} (u^\dagger \vec{\tilde{\alpha}})_{b'} |A_{u^\dagger a, b'}^{n-1}\rangle \right) \otimes \left(\sum_{c'} \tilde{\beta}_{c'} |A_{c'd}^{n-1}\rangle \right). \quad (24)$$

Note that since U is part of the $\text{SO}(3)$ symmetry of AKLT states, its action can be represented as a rotation of edge states through $u = e^{-i\pi\sigma_y/2}$ (see Sec. VIB). One can check by explicit computation that $u^\dagger \vec{\tilde{\alpha}} \parallel \vec{\tilde{\beta}}$, regardless of the initial state α_b and β_c or the type of quantum jump occurred in the previous attempt. Hence, the new state $|\psi'_1\rangle$ will have the maximum success probability of connection $p_{\max} = 1/2$, up to exponential corrections.

We now provide a more intuitive explanation on why success probability vanishes after any quantum jump, and why applying U works to restore the maximum success probability. We can interpret the dynamics under $\mathcal{L} = \mathcal{D}[c_\theta]$ as a continuous measurement of whether the pair of spins have $J_\theta = +2$, where $J_\theta = e^{-i\theta J_y} J_z e^{i\theta J_y}$. To be more specific, consider four spin-1 particles $\vec{S}_1, \dots, \vec{S}_4$, and imagine that we are performing a connection between site 2 and 3 by continuously measuring $\vec{J} = \vec{S}_2 + \vec{S}_3$. Now we “decompose” each spin-1 as if it is made out of two spin- $\frac{1}{2}$ particles: $\vec{S}_i = \vec{s}_{i,L} + \vec{s}_{i,R}$. It is known [4] that the AKLT state can be constructed by starting with singlet bonds of virtual spin- $\frac{1}{2}$ particles where $s_{i,R} + s_{i+1,L} = 0$, and then imposing the constraint that $s_{i,L} + s_{i,R} = 1$ are in one of the triplet states corresponding to the physical spin-1 states. The detection of a quantum jump c_θ in a failed connection attempt implies $J_\theta = 2$, which is only possible if $s_{2L}^\theta = s_{2R}^\theta = s_{3L}^\theta = s_{3R}^\theta = +\frac{1}{2}$. Due to the singlet bond conditions, this automatically implies $s_{1R}^\theta = s_{4L}^\theta = -\frac{1}{2}$. Subsequently, when we retry the connection with site 1 and 4, the overlap with the AKLT state is zero since the two virtual spin- $\frac{1}{2}$ particles are in the state $|s_{1R}^\theta = -\frac{1}{2}\rangle |s_{4L}^\theta = -\frac{1}{2}\rangle$ that has no overlap with the desired singlet bond state $|+\frac{1}{2}\rangle |-\frac{1}{2}\rangle - |-\frac{1}{2}\rangle |+\frac{1}{2}\rangle$. Now, applying U to one of the chains, say the first chain, flips s_{1R}^θ so that the resultant state is $|+\frac{1}{2}\rangle |-\frac{1}{2}\rangle$. This has overlap of $1/2$ with the singlet state, restoring our success probability to roughly $1/2$.

As stated in the main text, this protocol is robust against changes in the rotation axis; if the rotational axis deviates from the xy -plane by angle φ , then the above procedure to restore the success probability (by applying π -rotation around the new axis) yield a subsequent success probability of $\frac{1}{2} \cos^2 \varphi$.

C. Effect of imperfect quantum jump detection

In realistic experiments, the detection of quantum jumps often entails imperfections. The presence of such imperfections affects our protocol by (i) not heralding the failure of connection of two chains (false-positive), and (ii) incorrectly heralding failure when the connection has been successful (false-negative). The former may arise due to imperfect detection efficiency, and the latter due to the dark counts in the detector. As mentioned in the main text, our parallelized protocol can still have an efficient scaling even when such imperfect quantum jump detection is accounted for. In the false-negative scenario, we can still discard affected particle pairs and continue the procedure, but we have to adopt an ideal case success probability lower than p_{\max} (see below). To minimize the occurrence of false-positives, we propose two methods that address detector inefficiency. In the following analysis, let us denote the detector efficiency to be $1 - \eta$, the dark count rate r , and the ideal case success probability p .

Success probability after false-negative “failure”— We showed previously in Sec. VB that the maximum success probability of connection of $p_{\max} = 1/2$ can be recovered for the subsequent attempt after a failed connection (via detection of quantum jumps), if we discard the affected particles and apply a global π -rotation $U = e^{i\pi S_y}$ to one of the remaining chains. However, this is not the case if the quantum jump detector has only received a dark

count, i.e. the failure is a false-negative, and the connection has in fact succeeded. After a dark count is registered, the experimenter will unwittingly discard the particles at the original interface, apply U , and retry the connection anyways. If we consider the density matrix of the remaining pair of chains, we can see that their edge states at the interface are essentially randomized in a maximally mixed state, which would intuitively yield a success probability $p \approx 1/4$ in the attempt to connect them. More precisely, if k particles were discarded in each original chain of length n starting from interface (i.e. $2k$ particles in the middle of the connected chain of length $2n$), the success probability of connecting the two chains of length $n - k$ can be computed to be

$$p = \frac{1}{4}(1 - \epsilon^{2k}) + \mathcal{O}(\epsilon^n), \quad (25)$$

where $\epsilon = -1/3$. In particular, when $k = 1$, $p \simeq 2/9$.

Method 1— The first method to address false-positives from detector inefficiency is to only use jump operators of the form $c = |++\rangle\langle ++|$ for the connection. Once a quantum jump occurs, the state will continue to undergo quantum jumps indefinitely, creating a much larger signal and effectively larger detection efficiency. Consequently, the detector inefficiency can be exponentially suppressed by the time τ_c of having the jump operators turned on. Let τ_0 be the time-scale in which a single quantum jump would occur. In this case, the probability of diagnosing a successful connection and keeping the result is given by the probability of not detecting any quantum jumps over time τ_c

$$p_{\text{succ}} = \Pr\{\text{keep}\} = p(1 - r\tau_0)^{\tau_c/\tau_0} + (1 - p)\eta^{\tau_c/\tau_0} = p(1 - r\tau_0)^{\tau_c/\tau_0}(1 + a\tilde{\eta}^{\tau_c/\tau_0}), \quad (26)$$

where we denoted $a \equiv (1 - p)/p$ and $\tilde{\eta} = \eta/(1 - r\tau_0)$. The fidelity is the conditional probability that the diagnosed success was a truly successful connection

$$\mathcal{F} = \Pr\{\text{success}|\text{keep}\} = \frac{p(1 - r\tau_0)^{\tau_c/\tau_0}}{p(1 - r\tau_0)^{\tau_c/\tau_0} + (1 - p)\eta^{\tau_c/\tau_0}} = \frac{1}{1 + a\tilde{\eta}^{\tau_c/\tau_0}} \quad (27)$$

Note we can only achieve a fidelity arbitrarily close to 1 if $\tilde{\eta} < 1$, i.e. when the detector efficiency is larger than the dark count probability $1 - \eta > r\tau_0$. In order to achieve a final error of \mathcal{E} for a system size of n from initial chains of length n_0 , where n/n_0 connections are necessary, we need $1 - \mathcal{F} \leq n_0\mathcal{E}/n$, and consequently $\tau_c = \mathcal{O}(\ln(n/n_0\mathcal{E})/\ln\tilde{\eta}^{-1})$. This is consistent with the $\tau_c \sim \log n$ scaling necessary in the ideal protocol. Nonetheless, our new success probability now decreases with system size n as $p_{\text{succ}} \sim \mathcal{O}(n^{-\delta})$ if dark counts are non-negligible, where $\delta = \ln(1 - r\tau_0)/\ln\tilde{\eta} \approx r\tau_0/\ln\eta^{-1}$. Consider now the average time to prepare a chain of length n :

$$T(n) = T_0 + \frac{\tau_c + \tau_r(1 - p_{\text{succ}})}{p_{\text{succ}}} \log_2 \frac{n - n_c}{n_0 - n_c} \quad (28)$$

where $n_c = 2(1 - p_{\text{succ}})/p_{\text{succ}}$, T_0 is time to prepare initial length- n_0 chains, and τ_r is some constant time necessary to reset the edge states in the event of failure. On first sight, this would mean that our preparation time would ultimately scale polynomially instead of polylogarithmically in the infinite n limit. However, in the regime of $r\tau_0 \ll 1$, this polynomial dependence has a very small power, and its effect can be neglected if $r\tau_c \ll 1$. Hence, in practice, our protocol has an efficient, polylogarithmic scaling up to $n \ll n_{\text{max}} = \mathcal{O}((1/\eta)^{1/r\tau_0})$, beyond which it switches to a polynomial scaling. For instance, even if single-photon detection efficiency is $1 - \eta = 0.2$, then assuming a dark count rate of $r = 25$ Hz [5] and a quantum jump scattering rate of $\tau_0^{-1} \approx 1$ MHz, it takes an astronomically long chain of $n_{\text{max}} \sim 10^{4000}$ to reach the polynomial scaling. An example scaling under these conditions is shown in SFIG. 1 below.

Method 2— The second method for addressing detector inefficiency is to slowly turn on jump operators in the vicinity of the interface. In this way, the absence of quantum jumps further confirms that the two chains has indeed been successfully connected; since only a successful connection does not lead to any subsequent quantum jumps, any false-positive diagnosis of successful connection can be corrected. More concretely, consider a k -step scheme where we turn on jump operators to include k neighbors on each side of the original interface, one pair of neighbors at a time. At step $\ell = 1, \dots, k$, we have jump operators on for 2ℓ particles centered at the interface, turned on for time τ_ℓ^c . If a quantum jump occurred and evaded detection at any step ℓ , we assume τ_ℓ^c is long enough so that the 2ℓ particles would have formed a connected chain of length 2ℓ . At the subsequent step $\ell + 1$, the length- 2ℓ chain in the middle can be connected to the two length- $(n - \ell)$ chains on both sides if we succeed by having no quantum jump, producing a fully connected chain of length $2n$. Note the success probability for steps $\ell > 1$ is roughly $p_2 = 1/2^4$. From the system size scaling found in our numerical simulations presented in the main text, we expect to need $\tau_\ell^c \sim (2\ell)^{2.97} \approx (2\ell)^3$. Additionally, we expect the number of quantum jumps during τ_ℓ^c of step ℓ to roughly scale as $N_\ell^{\text{jump}} \approx C\tau_\ell^c$ for some constant C . Observe that this scheme allows us to obtain a fully connected chain even in the event of initial failure(s),

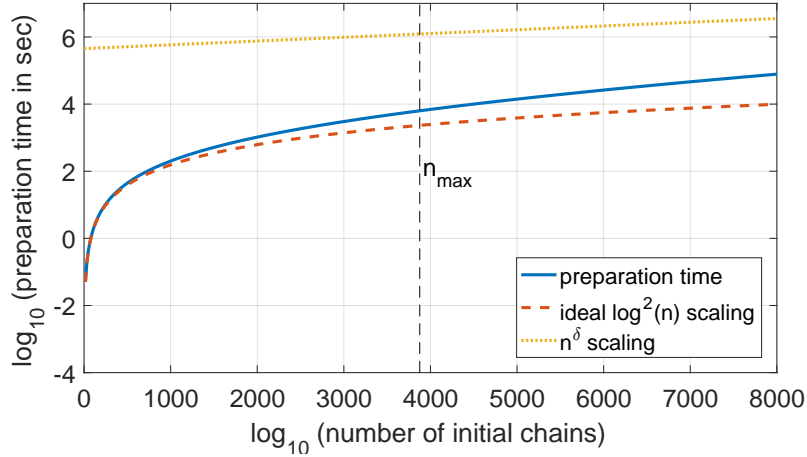


FIG. 1. Preparation time in the parallelized protocol with detector efficiency $1 - \eta = 0.2$ and dark count rate $r = 25$ Hz, using jump operators of the form $c = |++\rangle\langle ++|$ (Method 1). We also assume quantum jump rate $\tau_0^{-1} = 1$ MHz, ideal case success probability $p = 2/9$, time to discard atoms and reset edges $\tau_r = \tau_0$, and target final error $\mathcal{E} = 10^{-4}$.

as long as we don't have any quantum jumps at the last step. Thus, the probability of succeeding and deciding to keep the result (due to not detecting any quantum jump) is

$$\begin{aligned} \Pr\{\text{success and keep}\} &= pe^{-r \sum_{\ell=1}^k \tau_\ell^c} + (1-p)\eta^{C\tau_1^c} p_2 e^{-r \sum_{\ell=2}^k \tau_\ell^c} + (1-p)\eta^{C\tau_1^c} (1-p_2)\eta^{C\tau_2^c} p_2 e^{-r \sum_{\ell=3}^k \tau_\ell^c} + \dots \\ &= pe^{-rT_k} \left(1 + \frac{1-p}{p} p_2 \sum_{s=1}^{k-1} (1-p_2)^{s-1} (\eta^C e^r)^{T_s} \right), \end{aligned} \quad (29)$$

where $T_s = \sum_{\ell=1}^s \tau_\ell^c \approx Bs^4$ for some constant B . The probability of failing at the last step but still keeping the result is

$$\Pr\{\text{fail and keep}\} = (1-p)(1-p_2)^{k-1} \eta^{CT_k}. \quad (30)$$

The fidelity is the conditional probability of true success given that we have kept the result:

$$\begin{aligned} \mathcal{F} = \Pr\{\text{success}|\text{keep}\} &= \frac{pe^{-rT_k}(1+\dots)}{pe^{-rT_k}(1+\dots) + (1-p)(1-p_2)^{k-1} \eta^{CT_k}} \\ &\geq \frac{pe^{-rT_k}}{pe^{-rT_k} + (1-p)(1-p_2)^{k-1} \eta^{CT_k}} \approx 1 - b(1-p_2)^{k-1} \xi^{k^4}, \end{aligned} \quad (31)$$

where we denoted $b = (1-p)/p$ and $\xi = (\eta^C e^r)^B$. To achieve arbitrarily good fidelity, we require $\xi < 1$, i.e. the dark count rate $r < C \ln \eta^{-1}$ needs to be sufficiently small. At the same time, the apparent “success” probability of keeping the result is $p_{\text{succ}} = \Pr\{\text{keep}\} \approx pe^{-rBk^4}$. We can carry out the same analysis as in the previous method, and a similar behavior would emerge: when the dark count rate is nonzero, the efficient polylogarithmic scaling applies until a maximum chain length of $n \ll n_{\text{max}} = \mathcal{O}(\eta^{-C/r})$, beyond which a polynomial scaling of $\mathcal{O}(n^{\delta'})$ with $\delta' \approx r/\ln \eta^{-C}$ applies.

D. Scaling of imperfection in Rydberg-EIT implementation

Our protocol prepares AKLT states with finite fidelity when experimental imperfections are taken into account. Here, we analyze how fidelity scales as multiple chains are connected. In particular, the long-range nature of interaction in the proposed Rydberg-EIT implementation limits fidelity even in the absence of dephasing. Nevertheless, we show that by adopting the parallelized protocol, the long-range interactions only affect the initial preparation of length- n_0 chains, and such imperfection does not substantially grow in the later connection procedures. This is because the connections involve turning on the dissipative interaction on particle pairs that are spatially separated by at least n_0 particles. Since the effective decay rate scales as $\Gamma_{DD} \sim 1/R^{12}$ for the proposed implementation, the perturbative effect of long-range interaction is characterized by the very small number of $1/(n_0 - 1)^{12}$, which becomes even smaller

in later rounds of connections. Hence, we neglect the effect of long-range interaction on the connections, and only consider how the induced errors on the states of initial chains propagate through the protocol. Let us assume we initially start with individual chains of length n_0 , each with bounded error ϵ_0 . At the ℓ -th level of connections, we on average double the length $n_\ell \simeq 2n_{\ell-1} - n_c$, where n_c is the expected number of particles discarded in each connection. The number of initial chains necessary to reach a final chain length of n is $L = (n - n_c)/(n_0 - n_c)$, and $L - 1$ connection procedures need to be performed. Hence, the final error is bounded by

$$1 - \mathcal{F} \leq L\epsilon_0 + (L - 1) \times \mathcal{O}(e^{-\gamma_1 \tau_c}) \approx n\epsilon_0/n_0, \quad (32)$$

where we neglect the second term which can be made small compared to the first if we choose $\tau_c = \mathcal{O}(\ln n)$. As we can see, the predominant source of error is due to the imperfect initial chains, whose errors add linearly.

This linear scaling of error is indeed very favorable for *many-body state* preparation protocol. To put this in perspective, let us estimate how the effective temperature T_{eff} scales in our connection procedure. We define the effective temperature through the relation

$$\mathcal{F} = \text{tr} \left[P_G \frac{e^{-H/T_{\text{eff}}}}{\text{tr}[e^{-H/T_{\text{eff}}}]} \right] = \frac{1}{1 + \int_{\Delta_{\text{gap}}}^{\infty} \rho(E) e^{-E/T_{\text{eff}}} dE} \approx 1 - \int_{\Delta_{\text{gap}}}^{\infty} \rho(E) e^{-E/T_{\text{eff}}} dE, \quad (33)$$

where $\rho(E)$ is the density of state at energy E , and we assume that T_{eff} is sufficiently small. Now we consider connecting two length- n_1 chains at effective temperature T_1 (with errors $1 - \mathcal{F}_1$). After connection, we have a chain of length $n_2 \approx 2n_1$, with bounded error $1 - \mathcal{F}_2 \lesssim 2(1 - \mathcal{F}_1)$. Corresponding effective temperature T_2 of the connected chain can be estimated from

$$\begin{aligned} \int_{\Delta_{\text{gap}}}^{\infty} \rho_2(E) e^{-E/T_2} dE &\approx 1 - \mathcal{F}_2 \lesssim 2(1 - \mathcal{F}_1) \approx \int_{\Delta_{\text{gap}}}^{\infty} 2\rho_1(E) e^{-E/T_1} dE \\ \implies \int_{\Delta_{\text{gap}}}^{\infty} 2\rho_1(E) e^{-E/T_1} dE - \int_{\Delta_{\text{gap}}}^{\infty} \rho_2(E) e^{-E/T_2} dE &\gtrsim 0, \end{aligned}$$

where $\rho_1(E)$ and $\rho_2(E)$ denote the density of state for chains of length n_1 and $n_2 \approx 2n_1$, respectively. In a generic many-body interacting system, the density of state grows exponentially in system sizes. Here, we are most interested in the density of state of low-lying excitations, e.g. the first excited band, where the scaling of $\rho(E)$ can be much weaker. Ref. [6] used Bijl-Feynman single-mode approximation to deduce that there is a band of low-lying excited states with dispersion relation $E_1(k) = \frac{5}{27}(5 + 3 \cos k)$, corresponding to magnon excitations. Therefore, we expect the number of states in the low-lying excited bands to scale at least linearly with system size, and thus $\rho_2(E) \geq 2\rho_1(E)$. Applying this to the earlier inequality, we have

$$\int_{\Delta_{\text{gap}}}^{\infty} \rho_2(E) (e^{-E/T_1} - e^{-E/T_2}) dE \gtrsim 0 \implies T_2 \lesssim T_1. \quad (34)$$

Hence, the effective temperature should not increase (and can potentially decrease) after each connection procedure.

VI. GENERALIZATION

In this section, we generalize our protocol for a broader class of translation-invariant MPS with internal symmetry. We first introduce notations and a few useful known properties of translation-invariant MPS in Sec. VIA, which will be referenced in subsequent sections. More detailed description and proofs of these properties can be found in Ref. [1]. We then discuss the meaning of internal symmetry of MPS in Sec. VIB. Lastly, we define and analyze the generalization of our protocol in Sec. VIC and VID.

A. Notations and useful properties of matrix product states

Any (unnormalized) translation-invariant MPS with physical dimension d and bond dimension D can be written as:

$$|A_{ab}^n\rangle = \sum_{\{s_i\}} \langle a | A^{(s_1)} A^{(s_2)} \dots A^{(s_n)} | b \rangle | s_1 s_2 \dots s_n \rangle, \quad (35)$$

where $s_i \in \{1, 2, \dots, d\}$ runs over the physical spin basis for the i -th particle, and $|a\rangle, |b\rangle \in \mathbb{C}^D$ indicate the ‘‘boundary conditions’’ on the virtual bond level. We use the notation $|A_{ab}^n\rangle$ to indicate translational-invariant MPS of n particles

with open boundary condition specified by a and b , and $|A^n\rangle$ to denote the state of a n -particle system with periodic boundary condition, i.e. $|A^n\rangle = \sum_a |A^n_{aa}\rangle$. For the case of AKLT states, we have $d = 3$ and $D = 2$. Under open boundary condition, there could be at most D^2 distinct states with different possible boundary conditions, e.g. four-fold degeneracy of AKLT states. In general, however, these D^2 states may not be linearly independent unless the MPS is *injective* (defined below).

Canonical Form— An MPS is in a *canonical form* if the matrices have a common block diagonal structure: $A^{(s)} = \text{diag}(\lambda_1 A_1^{(s)}, \dots, \lambda_B A_B^{(s)})$, where $0 < \lambda_\beta \leq 1$ for each block $\beta \in \{1, \dots, B\}$. The matrices in each block must satisfy the conditions that (i) $\sum_s A_\beta^{(s)} A_\beta^{(s)\dagger} = \mathbb{1}$, (ii) a map defined as $\mathcal{E}_\beta(X) = \sum_s A_\beta^{(s)} X A_\beta^{(s)\dagger}$ has $\mathbb{1}$ as its only fixed point (unique eigenvector with unity eigenvalue), and finally (iii) $\sum_s A_\beta^{(s)\dagger} \Lambda_\beta A_\beta^{(s)} = \Lambda_\beta$ for some diagonal positive and full-rank matrices Λ_β .

Transfer Matrix— Consider the completely positive map $\mathcal{E}(X) = \sum_s A^{(s)} X A^{(s)\dagger}$, or equivalently the transfer matrix $T = \sum_s A^{(s)*} \otimes A^{(s)}$. Understanding the spectrum of this map is useful for computing the expectation value of an observable or the overlap between two quantum states, e.g. $\langle A^n_{ab} | A^n_{a'b'} \rangle = \langle aa' | T^n | bb' \rangle$ [1]. Some eigenvectors of T are $\frac{1}{\sqrt{D_\beta}} \sum_{i \in \beta} |ii\rangle$, where D_β is the dimension of the β -th block, and correspond to eigenvalues $|\lambda_\beta|^2$. Denoting the other eigenvectors of T with eigenvalues ϵ_ν as $|\nu\rangle$, we have

$$\langle A^n_{ab} | A^n_{a'b'} \rangle = \langle aa' | \left[\sum_\beta \frac{|\lambda_\beta|^2}{D_\beta} \sum_{i,j \in \beta} |ii\rangle \langle jj| + \sum_\nu \epsilon_\nu |\nu\rangle \langle \nu| \right]^n | bb' \rangle = \sum_\beta \frac{|\lambda_\beta|^{2n}}{D_\beta} \delta_{a,b \in \beta} \delta_{aa'} \delta_{bb'} + \sum_\nu \epsilon_\nu^n \langle aa' | \nu \rangle \langle \nu | bb' \rangle. \quad (36)$$

Since $|\lambda_\beta|^2$ is the largest eigenvalue of each block β , typically only the first term is relevant in the limit of large n .

Parent Hamiltonian— For a sufficiently large L , the set of matrix products $\{A^{(s_1)} \dots A^{(s_L)} : 1 \leq s_i \leq d\}$ spans the vector space of all matrices with the same block diagonal structure as the canonical form [1]. We call L the *interaction length* of the MPS. Without loss of generality, we can assume that $L = 2$. This is because otherwise we can group L sites together to get an equivalent MPS with larger physical dimension $d' \leq d^L$, and a new interaction length $L' = 2$. The *parent Hamiltonian* of an MPS is then defined to be $H_p = \sum_i h^{(i)}$, where h is any positive semi-definite operator acting on nearest neighboring sites, whose kernel is

$$\ker(h) = \text{span}\{|A_{ab}^2\rangle : \forall a, b\}. \quad (37)$$

In other words, H_p imposes a condition $h^{(i)}$ for every pair of neighboring sites $(i, i+1)$, which our MPS trivially verifies (i.e. $h^{(i)} |A_{ab}^n\rangle = 0$ for all $1 \leq i \leq n-1$). Hence, H_p is a frustration-free Hamiltonian of which the MPS is a zero-energy ground state. The ground state degeneracy depends on both the boundary condition and the number of blocks in the MPS canonical form. Ref. [1] has shown that under periodic boundary condition, this degeneracy equals the number of independent blocks in the canonical form, since the ground space consists of MPS constructed from the sub-matrices from every block.

Injectivity— Often it is useful to assume a condition that the MPS is *injective*, which is satisfied in the generic case except for specific, fine-tuned MPS [1]. This injectivity condition is that the transfer matrix T has only one eigenvector corresponding to its largest eigenvalue (which we normalize to 1 in the canonical form). This also implies that there is just one block in the canonical form of the MPS. In this case,

$$\langle A^n_{ab} | A^n_{a'b'} \rangle = \langle aa' | T^n | bb' \rangle = \frac{1}{D} \delta_{aa'} \delta_{bb'} + \mathcal{O}(\epsilon_2^n), \quad (38)$$

where ϵ_2 is the second largest eigenvalue of \mathcal{E} . Additionally, this implies that the parent Hamiltonian under periodic boundary condition has the MPS as its unique ground state, and that the ground state energy is gapped in the thermodynamic limit. Under open boundary condition, D^2 distinct boundary conditions give rise to D^2 linearly independent and degenerate ground states $|A^n_{ab}\rangle$. By appropriately modifying the parent Hamiltonian terms at the boundaries, we can break the degeneracy and make one of the D^2 states the unique ground state.

B. Internal Symmetries of MPS

We say a translation-invariant MPS defined on d -level physical spins respects an internal symmetry \mathcal{G} , if for some unitary representation $U : \mathcal{G} \rightarrow U(d)$, we have:

$$U_g^{\otimes n} |A^n_{ab}\rangle = \sum_{a'b'} [\chi_g]_{ab}^{a'b'} |A^n_{a'b'}\rangle \quad \text{and} \quad U_g^{\otimes n} |A^n\rangle = e^{i\theta_g} |A^n\rangle. \quad (39)$$

That is, a global action of the symmetry operation keeps a ground state of the MPS parent Hamiltonian in the ground space under open boundary condition, or only imprints a complex phase factor under periodic boundary condition.

Assuming the symmetry group is reasonable (either discrete or a compact connected Lie group), but without assuming injectivity, Ref. [7] showed that we can replace the action of the symmetry in the physical basis with a unitary in the virtual bond basis. More explicitly, we have

$$\sum_{s'} [U_g]_{ss'} A^{(s')} = w_g u_g A^{(s)} u_g^\dagger, \quad (40)$$

where $u_g = P_g v_g$, with $v_g = \bigoplus_{\beta=1}^B v_g^\beta$ taking on the same block diagonal structure as $A^{(s)}$, and each v_g^β a unitary in block β . P_g is a permutation amongst blocks. Lastly, $w_g = \bigoplus_{\beta} e^{i\varphi_g^\beta} \mathbf{1}_\beta$ is a phase factor for each block. If \mathcal{G} is a compact connected Lie group, Ref. [7] showed that $P_g = \mathbf{1}$, while $g \mapsto e^{i\varphi_g^\beta}$ and $g \mapsto v_g^\beta$ are representations of \mathcal{G} .

For AKLT states, where $\mathcal{G} = \text{SO}(3)$, the relevant representation is given by the rotations $U_g = \exp(i\vec{\alpha}_g \cdot \vec{S})$ on the spin-1 vector \vec{S} for some real parameters $\vec{\alpha}_g = (\alpha_g^x, \alpha_g^y, \alpha_g^z)$. In particular, we have

$$\sum_{s'} [U_g]_{ss'} A^{(s')} = u_g A^{(s)} u_g^\dagger \implies U_g^{\otimes n} |A_{ab}^n\rangle = |A_{u_g^\dagger a, u_g^\dagger b}^n\rangle, \quad (41)$$

where $u_g = \exp(i\vec{\alpha}'_g \cdot \vec{\sigma}/2)$, where $\vec{\alpha}'_g = (\alpha_g^x, -\alpha_g^y, \alpha_g^z)$.

C. Generalization of our protocol

In this section, we generalize our protocol to any translation-invariant MPS with internal symmetry \mathcal{G} . Our goal is to design a dissipative dynamics that deterministically prepares the ground state(s) of the MPS parent Hamiltonian using a set of global coherent manipulations and a minimal number k_{\min} of jump operators $\{c_1, c_2, \dots, c_{k_{\min}}\}$, each of the form $c_\mu = |\phi_\mu\rangle\langle\psi_\mu|$ acting on neighboring pairs of particles.

Without loss of generality, we assume that the desired states are ground states of a gapped, frustration-free parent Hamiltonian $H_p = \sum_i h^{(i)}$, where $h^{(i)}$ is a translation-invariant, nearest-neighbor projector that respects the internal symmetry \mathcal{G} [1, 7]. Each term h can be written in a block diagonal form, corresponding to different irreducible representations of \mathcal{G} . We denote the two-particle subspace that h projects onto as ‘‘bright manifold’’ $\mathfrak{B} \equiv \text{range}(h) \subset \mathbb{C}^{d^2}$. The ground states are uniquely characterized by vanishing populations in \mathfrak{B} . In the H_{AKLT} example, \mathfrak{B} corresponds to the $J = 2$ manifold of two neighboring spins. Similar to our protocol for AKLT, we can depopulate \mathfrak{B} by employing jump operators c_μ where $\text{range}(c_\mu^\dagger c_\mu) \subseteq \mathfrak{B}$. The number of jump operators can be reduced by utilizing and averaging over all symmetry rotations through $c_\mu \mapsto V_g^\dagger c_\mu V_g$, where V_g is the global unitary rotation by a group element $g \in \mathcal{G}$. Unlike in the AKLT case, the representation of \mathcal{G} on \mathfrak{B} may contain multiple copies of isomorphic irreducible representations in general. In such cases, the averaging of a single jump operator c_μ over \mathcal{G} may not be sufficient to depopulate the entire subspace \mathfrak{B} , and it becomes necessary to employ a set of multiple c_μ 's.

The foremost necessary condition for the jump operators c_μ is

$$\mathfrak{B} = \text{range} \left(\sum_{\mu=1}^{k_{\min}} Q_\mu \right) \quad \text{where} \quad Q_\mu = \frac{1}{|\mathcal{G}|} \sum_{g \in \mathcal{G}} V_g^\dagger c_\mu^\dagger c_\mu V_g = \frac{1}{|\mathcal{G}|} \sum_{g \in \mathcal{G}} V_g^\dagger |\psi_\mu\rangle\langle\psi_\mu| V_g. \quad (42)$$

In other words, the jump operators must be capable of depopulating the entire bright manifold after averaging over all symmetry operations. While here we have assumed the symmetry group \mathcal{G} is finite for simplicity, the following results apply to any compact group by replacing the sum over $g \in \mathcal{G}$ by an integral over the Haar measure of \mathcal{G} .

To find the minimum number k_{\min} of $|\psi_\mu\rangle$ (and consequently c_μ) required, it is useful to decompose V_g into direct sums of irreducible representations (irreps) $V_g = \bigoplus_r V_g^r$, where r enumerates the irreps, each with dimension d_r . This decomposition is possible because finite-dimensional unitary representations of any group are completely reducible [8]. Let us also denote $|\psi_\mu\rangle = \bigoplus_r |\psi_\mu^r\rangle$, where each $|\psi_\mu^r\rangle$ is a d_r -dimensional vector. Observe that for any $d_r \times d_{r'}$ matrix X , we can derive the following identity using Schur's Lemma [8]:

$$\frac{1}{|\mathcal{G}|} \sum_{g \in \mathcal{G}} V_g^r X V_g^{r'\dagger} = \begin{cases} 0 & \text{if } r \neq r' \\ \frac{\text{tr}(U_{rr'}^\dagger X)}{d_r} U_{rr'} & \text{if } r \cong r', \text{ i.e. } V_g^r = U_{rr'} V_g^{r'} U_{rr'}^\dagger \end{cases}, \quad (43)$$

where $r \cong r'$ means r is equivalent (isomorphic) to r' up to a unitary basis change. Note we can always choose a basis for the representation of V_g that absorbs $U_{rr'}$, so we assume $U_{rr'} = \mathbb{1}$ without loss of generality. Using the notation $\bigoplus_{r,r'} M_{r,r'}$ to denote the matrix whose (r, r') th block is $M_{r,r'}$, we can write Q_μ through the above identity

$$Q_\mu = \bigoplus_{r,r'} \frac{1}{|\mathcal{G}|} \sum_{g \in \mathcal{G}} V_g^r |\psi_\mu^r\rangle \langle \psi_\mu^{r'}|^\dagger V_g^{r'\dagger} = \bigoplus_r \frac{\mathbb{1}_r}{d_r} \langle \psi_\mu^r | \psi_\mu^r \rangle + \bigoplus_{r \neq r', r \cong r'} \frac{\mathbb{1}_r}{d_r} \langle \psi_\mu^{r'} | \psi_\mu^r \rangle, \quad (44)$$

where the second term characterizes the possible non-zero off-diagonal blocks, which can only exist between pairs of equivalent irreps.

Since inequivalent irreps are decoupled, we for now only consider the subspace $\mathfrak{B}_r \subseteq \mathfrak{B}$ corresponding to K_r copies of irreps equivalent to irrep r ($\dim \mathfrak{B}_r = K_r d_r$). We shall also denote $Q_\mu^r = Q_\mu|_{\mathfrak{B}_r}$ as the operator Q_μ restricted to the subspace \mathfrak{B}_r . Observe that $|\psi_\mu\rangle$ restricted to this subspace is specified by the set of K_r vectors $\{|\psi_\mu^s\rangle \in \mathbb{C}^{d_r}\}_{s=1}^{K_r}$. When $K_r > d_r$, regardless of the choice of $|\psi_\mu\rangle$, there are $K_r - d_r$ linearly independent vectors $\vec{\beta}^j \in \mathbb{C}^{K_r}$, $j = 1, \dots, K_r - d_r$, such that $\sum_{s=1}^{K_r} \beta_s^j \langle \psi_\mu^s | = 0$. Then any vectors of the form $|\chi\rangle = \bigoplus_{s=1}^{K_r} \beta_s^j |v\rangle$ are in the kernel of Q_μ^r for any $|v\rangle \in \mathbb{C}^{d_r}$, since one can verify $Q_\mu^r |\chi\rangle = 0$. Since there are $(K_r - d_r)d_r$ linearly independent such vectors $|\chi\rangle$, we have $\text{rank}(Q_\mu^r) \leq d_r^2$. Hence, in order to fully depopulate \mathfrak{B}_r , we need $\dim(\mathfrak{B}_r) = \text{rank}(\sum_\mu Q_\mu^r) \leq \sum_\mu \text{rank}(Q_\mu^r) \leq k_{\min} d_r^2$. Because k_{\min} must be an integer, we must have $k_{\min} \geq \lceil K_r/d_r \rceil$.

Note that this lower bound for k_{\min} can be saturated by construction. First, we partition the K_r equivalent irreps into $\lceil K_r/d_r \rceil$ groups of no more than d_r irreps. For each group, we can assign a $|\psi_\mu\rangle$ that is nonzero only in the subspace corresponding to the irreps in the group. Lastly, we make all off-diagonal blocks vanish for each group $\mu \in \{1, \dots, \lceil K_r/d_r \rceil\}$, by finding $\leq d_r$ mutually orthogonal vectors $|\psi_\mu^{r'}\rangle \in \mathbb{C}^{d_r}$ such that $\langle \psi_\mu^{r'} | \psi_\mu^r \rangle = 0$ for $r \neq r'$. For a single jump operator of the form $c_\mu = |\phi_\mu\rangle \langle \psi_\mu|$, the state $|\psi_\mu\rangle$ may have supports on more than one subspaces \mathfrak{B}_r . Therefore, the construction of a set of jump operators $\{c_\mu\}$ to satisfy Eq. (42) can be done in ‘‘parallel’’ for all the different \mathfrak{B}_r corresponding to the inequivalent set of irreps, leading to the minimum number

$$k_{\min} = \max_r \lceil K_r/d_r \rceil. \quad (45)$$

Here, r enumerates inequivalent irreps of \mathcal{G} in \mathfrak{B} , K_r is the number of copies of r , and d_r is the dimension of r .

We can also consider arbitrary jump operator c_μ beyond the rank-1 form of $|\phi_\mu\rangle \langle \psi_\mu|$. For any operator c_μ , we can perform singular value decomposition to write $c_\mu = \sum_{i_\mu} \sqrt{\gamma_{i_\mu}} |\phi_{i_\mu}\rangle \langle \psi_{i_\mu}|$, where $\langle \phi_{i_\mu} | \phi_{j_\mu} \rangle = \langle \psi_{i_\mu} | \psi_{j_\mu} \rangle = \delta_{i_\mu j_\mu}$. Then $c_\mu^\dagger c_\mu = \sum_{i_\mu} \gamma_{i_\mu} |\psi_{i_\mu}\rangle \langle \psi_{i_\mu}|$ with $\gamma_{i_\mu} > 0$. Hence, the condition of Eq. (42) becomes a condition imposed on the set of right-singular vectors $\{|\psi_{i_\mu}\rangle : \forall \mu, i_\mu\}$, where we must have $\mathfrak{B} = \text{range}(\frac{1}{|\mathcal{G}|} \sum_{g,\mu,i_\mu} \gamma_{i_\mu} V_g^\dagger |\psi_{i_\mu}\rangle \langle \psi_{i_\mu}| V_g)$. We can thus apply the k_{\min} found for rank-1 jump operators as the minimum number of independent $|\psi_{i_\mu}\rangle$'s.

Once we construct a set of c_μ 's satisfying the necessary condition of Eq. (42), it remains to ascertain the uniqueness of steady states using our inductive proof strategy. In other words, one simply need to check whether there are non-trivial solutions to Eq. (9) and (12) for open and periodic boundary conditions. Nevertheless, for non-injective MPS, this scheme cannot break the ground state degeneracy intrinsic to the MPS parent Hamiltonian, but it can guarantee the ground states are the only non-decaying steady states.

D. Parallelized protocol for general case

In this section, we consider generalization of our parallelized protocol to prepare a translation-invariant MPS with bond dimension D and internal symmetry \mathcal{G} . We assume that the MPS is injective for simpler analysis. Consider an arbitrary initial state of two length- n chains of MPS, which can be written as $|\psi_0\rangle = \mathcal{N}_0 \sum_{b,c} C_{bc} |A_{ab}^n\rangle \otimes |A_{cd}^n\rangle$, where $C_{bc} \in \mathbb{C}^{D \times D}$ is some arbitrary coefficient matrix that characterizes the edge states at the interface of the chains, and \mathcal{N}_0 is normalization constant. If we have an initially unentangled pair of chains, we must have $C_{bc} = \alpha_b \beta_c$ for some $\vec{\alpha}, \vec{\beta} \in \mathbb{C}^D$. By turning on the jump operators acting at the interface, we can cool this state into the desired final state $|\psi_f^{2n}\rangle = \mathcal{N}_f |A_{ad}^{2n}\rangle$. Since the MPS is assumed to be injective, we can use Eq. (38) to find the success probability (of undergoing no quantum jumps for a sufficiently long time)

$$p \simeq |\langle \psi_f^{2n} | \psi_0 \rangle|^2 = \frac{|\text{tr}[C]|^2}{D \text{tr}[C^\dagger C]} + \mathcal{O}(\epsilon_2^n) = \frac{|\vec{\alpha} \cdot \vec{\beta}|^2}{D |\vec{\alpha}|^2 |\vec{\beta}|^2} + \mathcal{O}(\epsilon_2^n) \quad \text{if } C_{bc} = \alpha_b \beta_c, \quad (46)$$

where we wrote the expression in a more suggestive form assuming initially unentangled chains. For random states $\vec{\alpha}, \vec{\beta} \in \mathbb{C}^D$, we have on average $p \simeq 1/D^2$. The maximum success probability of $p_{\max} = 1/D$ is obtained when

$\vec{\alpha} \parallel \vec{\beta}$, i.e. when the two edge states are identical. Hence, there is a system-size-independent success probability if we attempt to connect two chains of injective MPS by turning on the jump operators for the two particles at the interface. Consequently, we can improve the scaling of preparation time of our desired MPS by connecting many pairs of chains in parallel in the same way as proposed for AKLT.

When our desired MPS also exhibits bond-inversion symmetry \mathcal{P} like AKLT, we have the same issue of vanishing success probability after a quantum jump that also respects \mathcal{P} . In the event of a quantum jump due to a jump operator of the form $c = |\phi\rangle\langle\psi|$, the state after discarding the two particles at the interface is $|\psi_1\rangle = \mathcal{N}_1 \sum_{b',c'} \tilde{C}_{b'c'} |A_{ab'}^{n-1}\rangle |A_{c'd'}^{n-1}\rangle$, where

$$\tilde{C}_{b'c'} = \sum_{bc} \langle\psi| (|A_{b'b}^1\rangle \otimes |A_{c'c'}^1\rangle) C_{bc}. \quad (47)$$

If $|\psi\rangle$ respects bond-inversion symmetry, i.e. $\mathcal{P}|\psi\rangle = \pm|\psi\rangle$, where $\mathcal{P} = \sum_{i,j} |ij\rangle\langle ji|$, then

$$\text{tr}[\tilde{C}] = \sum_a \tilde{C}_{aa} = \sum_{abc} \langle\psi| (|A_{ab}^1\rangle \otimes |A_{ca}^1\rangle) C_{bc} = \sum_{abc} \langle\psi| \mathcal{P} (|A_{ca}^1\rangle \otimes |A_{ab}^1\rangle) C_{bc} = \sum_{bc} \pm \langle\psi| A_{cb}^2 \rangle C_{bc} = 0. \quad (48)$$

We find that this quantity is zero regardless of initial C_{bc} , entangled or unentangled, due to our requirement that $|\psi\rangle$ be orthogonal to the desired MPS states $|A_{cb}^2\rangle$. In fact, $\text{tr}[\tilde{C}]$ is related to the success probability of the next connection attempt: $p' \simeq \left| \langle\psi_f^{2n-2} | \psi_1 \rangle \right|^2 \propto |\text{tr}[\tilde{C}]|^2 + \mathcal{O}(\epsilon_2^n) = \mathcal{O}(\epsilon_2^n)$, which is exponentially small for a large system size.

Similar to the AKLT case, we can also try to restore the success probability by applying a global symmetry operation $U_g^{\otimes n-1}$ for some $g \in \mathcal{G}$ to one of the chains. In our AKLT protocol, there is a symmetry operation $U = e^{i\pi S_y}$ whose action on the virtual bond level $u = e^{-i\pi\sigma_y/2}$ yields $|\text{tr}[u^\dagger \tilde{C}]|^2 = \text{tr}[\tilde{C}^\dagger \tilde{C}]$, allowing us to recover the maximum success probability of $p_{\max} = 1/D$ regardless of initial state C_{bc} or which quantum jump occurred. While the existence of such an operation is not known for the general case, we can at least restore the success probability to $1/D^2$ for many injective MPS by applying a randomly chosen symmetry operation. This is because the $\{A^{(s)}\}$ matrices that generate the MPS only has one block if it is injective, and hence the symmetry operation represented on the virtual bond space u_g can be one irreducible representation of dimension D . A sufficient condition for irreducibility of u_g is given in Ref. [7], which is that U_g be irreducible and $\{A^{(s)\dagger} A^{(s')}\} : \forall s, s'\}$ spans the whole space of matrices. When u_g is irreducible, applying a global symmetry operation $U_g^{\otimes n-1}$ randomly chosen from the group would change any edge state $|b\rangle$ to $\frac{1}{|\mathcal{G}|} \sum_{g \in \mathcal{G}} u_g^\dagger |b\rangle \langle b| u_g = \mathbf{1}/D$. This will then yield a subsequent success probability of $1/D^2$.

Non-injective case— The analysis of generalization to non-injective cases is more subtle. Here we consider an example to prepare GHZ states: $|\text{GHZ}_\pm\rangle = (|0^n\rangle \pm |1^n\rangle)/\sqrt{2}$, which has an MPS representation with $(d, D) = (2, 2)$ given by the following matrices:

$$A^{(0)} = |\uparrow\rangle\langle\uparrow| = \begin{pmatrix} 1 & 0 \\ 0 & 0 \end{pmatrix} \quad \text{and} \quad A^{(1)} = |\downarrow\rangle\langle\downarrow| = \begin{pmatrix} 0 & 0 \\ 0 & 1 \end{pmatrix}. \quad (49)$$

Note this is in a canonical form, with two one-dimensional blocks. In this representation, $|\text{GHZ}_+\rangle \propto |A_{\rightarrow\rightarrow}^n\rangle = |A_{\leftarrow\leftarrow}^n\rangle$, and $|\text{GHZ}_-\rangle \propto |A_{\rightarrow\leftarrow}^n\rangle = |A_{\leftarrow\rightarrow}^n\rangle$, where $|\rightarrow\rangle = (|\uparrow\rangle + |\downarrow\rangle)/\sqrt{2}$ and $|\leftarrow\rangle = (|\uparrow\rangle - |\downarrow\rangle)/\sqrt{2}$ are possible edge configurations. This MPS has an internal symmetry group of $\mathcal{G} = \mathbb{Z}_2$, which is represented by $\{\mathbf{1}, \sigma_x^{\otimes n}\}$ acting on the system. Its parent Hamiltonian is $H_{\text{GHZ}} = \sum_i (\mathbf{1} - \sigma_z^{(i)} \sigma_z^{(i+1)})$, whose ground states are doubly degenerate due to non-injectivity. The corresponding two-particle bright manifold is $\mathfrak{B} = \text{span}\{|\Phi_+\rangle, |\Phi_-\rangle\}$, where $|\Phi_\pm\rangle = (|01\rangle \pm |10\rangle)/\sqrt{2}$. The two states $|\Phi_\pm\rangle$ support two distinct irreducible representations of \mathbb{Z}_2 , which are respectively the trivial and the sign representation. Hence, we can use just one jump operator of the form e.g. $c = |00\rangle (\kappa_+ \langle\Phi_+| + \kappa_- \langle\Phi_-|)$, $\kappa_\pm \neq 0$, along with the global symmetry operation $\sigma_x^{\otimes n}$, to depopulate the bright manifold and obtain $\text{span}\{|\text{GHZ}_\pm\rangle\}$ as the subspace of steady states. Now let us consider preparing $|\text{GHZ}_\pm\rangle$ in a parallelized protocol with connections and feedback. We note that unlike in the injective case, different choices of jump operator here can lead to qualitatively different outcomes. Specifically, we consider two choices of jump operators that may result in different degrees of entanglement of the final state. Firstly, consider an example choice of the jump operator $c = |00\rangle\langle 01|$ (i.e. $\kappa_\pm = 1/\sqrt{2}$). While this along with the symmetry operation produces a dissipative dynamics that has $|\text{GHZ}_\pm\rangle$ as the unique steady states, the parallelized protocol can only produce an unentangled final state of either $|0^n\rangle \propto |\text{GHZ}_+\rangle + |\text{GHZ}_-\rangle$ or $|1^n\rangle \propto |\text{GHZ}_+\rangle - |\text{GHZ}_-\rangle$ once any quantum jump occurs, regardless of states of the initial chains. Alternatively, we choose the jump operator $c = |00\rangle (\langle 01| + i \langle 10|)/\sqrt{2}$ (i.e. $\kappa_+ = \kappa_-^* = (1+i)/2$). In this case, suppose we start with $|0^{n_0}\rangle + |1^{n_0}\rangle$ on the initial length- n_0 chains, then we can produce a maximally entangled final state of $|0^n\rangle + \zeta |1^n\rangle$ even after quantum jumps, for some $\zeta \in \{\pm 1, \pm i\}$. In both cases, for arbitrary (unentangled) initial

states $|\psi_0\rangle = \sum_{a,b=0}^1 (\alpha_a |a^n\rangle) \otimes (\beta_b |b^n\rangle)$ of two chains, the success probability of connecting them is on average $1/2$ for random $\vec{\alpha}, \vec{\beta} \in \mathbb{C}^2$. Note that this success probability is maximally 1, e.g. if the initial state is $|0^n\rangle \otimes |0^n\rangle = |0^{2n}\rangle$.

- [1] D. Perez-Garcia, F. Verstraete, M. M. Wolf, and J. I. Cirac, *Quantum Inf. Comput.* **7**, 401 (2007).
- [2] B. Kraus, H. P. Büchler, S. Diehl, A. Kantian, A. Micheli, and P. Zoller, *Phys. Rev. A* **78**, 042307 (2008).
- [3] F. Reiter and A. S. Sørensen, *Phys. Rev. A* **85**, 032111 (2012).
- [4] I. Affleck, T. Kennedy, E. H. Lieb, and H. Tasaki, *Phys. Rev. Lett.* **59**, 799 (1987).
- [5] R. H. Hadfield, *Nature Photonics* **3**, 696 (2009).
- [6] D. P. Arovas, A. Auerbach, and F. D. M. Haldane, *Phys. Rev. Lett.* **60**, 531 (1988).
- [7] M. Sanz, M. M. Wolf, D. Pérez-García, and J. I. Cirac, *Phys. Rev. A* **79**, 042308 (2009).
- [8] M. Artin, “Algebra,” (Pearson, 2010) Chap. 10, pp. 290–322, 2nd ed.